

1969

# Green's function formulation of Laplace transformed multigroup diffusion equations

Michael Richard Ringham  
*Iowa State University*

Follow this and additional works at: <https://lib.dr.iastate.edu/rtd>

 Part of the [Nuclear Engineering Commons](#), and the [Oil, Gas, and Energy Commons](#)

## Recommended Citation

Ringham, Michael Richard, "Green's function formulation of Laplace transformed multigroup diffusion equations " (1969).  
*Retrospective Theses and Dissertations*. 4145.  
<https://lib.dr.iastate.edu/rtd/4145>

This Dissertation is brought to you for free and open access by the Iowa State University Capstones, Theses and Dissertations at Iowa State University Digital Repository. It has been accepted for inclusion in Retrospective Theses and Dissertations by an authorized administrator of Iowa State University Digital Repository. For more information, please contact [digirep@iastate.edu](mailto:digirep@iastate.edu).

70-13,625

RINGHAM, Michael Richard, 1940-  
GREEN'S FUNCTION FORMULATION OF LAPLACE  
TRANSFORMED MULTIGROUP DIFFUSION EQUATIONS.

Iowa State University, Ph.D., 1969  
Engineering, nuclear

**University Microfilms, Inc., Ann Arbor, Michigan**

THIS DISSERTATION HAS BEEN MICROFILMED EXACTLY AS RECEIVED

GREEN'S FUNCTION FORMULATION OF LAPLACE  
TRANSFORMED MULTIGROUP DIFFUSION EQUATIONS

by

Michael Richard Ringham

A Dissertation Submitted to the  
Graduate Faculty in Partial Fulfillment of  
The Requirement: for the Degree of  
DOCTOR OF PHILOSOPHY

Major Subject: Nuclear Engineering

Approved:

Signature was redacted for privacy.

In Charge of Major Work

Signature was redacted for privacy.

Head of Major Department

Signature was redacted for privacy.

Dean of Graduate College

Iowa State University  
Ames, Iowa

1969

## TABLE OF CONTENTS

	Page
I. INTRODUCTION	1
II. LITERATURE SURVEY	3
III. THEORETICAL DEVELOPMENT	5
A. Analytic Considerations	5
B. Numerical Considerations	19
C. Numerical Inversion	29
IV. APPLICATION AND MODEL USED	33
V. RESULTS AND DISCUSSION	42
VI. TOPICS FOR FURTHER STUDY	59
VII. LITERATURE CITED	60
VIII. ACKNOWLEDGMENTS	62

## I. INTRODUCTION

The space and time dependent diffusion equations, while only an approximation to the more complex transport equation, still can not be solved in their general form. They present a coupled set of partial differential equations with coefficients which are not, in general, continuous functions of position. Since an exact solution can not be obtained, the only recourse is approximation techniques.

The rapidly expanding computer technology with increased core space and faster execution times provides opportunities to explore a variety of techniques which would previously have been out of the question. Brute force techniques of old, which had been put aside for more sophisticated mathematics, are being implemented to yield powerful tools in the solution of difficult problems. Separation of variables and finite difference approaches have been used frequently to determine space-time solutions to the multigroup diffusion equations. While the results obtained from these techniques are encouraging, it would seem that other methods should be explored.

The object of this investigation is to determine the feasibility of obtaining space-time solutions to the multigroup diffusion equations by taking the Laplace transform with respect to time. This leaves a set of ordinary differential equations in space involving the Laplace transform

variable  $s$ . The reduced set of equations is solved for discrete values of  $s$  consistent with the numerical scheme to be utilized in returning to the time domain. The inversion technique utilized is one presented by Bellman et al. (1) in a text on numerical inversion from the Laplace transform domain.

A Green's function approach was chosen as the means of determining the space dependent  $s$  domain solution. Conventional numerical techniques were utilized in evaluating the integrals arising from the formulation. Delayed neutrons were not considered but there would be little difficulty extending the method to include them.

A program was written to test the method and the results obtained are compared to WIGLE-40. There was no attempt to optimize the program in terms of computer calculation time or solution accuracy. There are many variables in the method which could affect both the speed and accuracy of the program and there is no reason to believe that either or both could not be improved. Some suggestions along this line are included in topics for further study.

## II. LITERATURE SURVEY

Recent space-time work centers around two basic approaches, modal analysis and numerical solutions. Modal analysis is characterized by the generation of an approximate solution by means of a finite series of space modes with time dependent coefficients. Once the space modes have been chosen, the problem becomes one of determining the best set of time coefficients. The number of modes necessary to obtain a good approximation depends strongly on the perturbation considered.

A number of the modal approaches utilize orthogonal space modes (2, 3, 4, 5). The orthogonality is utilized in the determination of the time coefficients. Another modal approach utilizes Green's function modes (6, 7, 8, 9, 10). The diffusion equations are written in an integral form with a space and time dependent Green's function kernel which is subsequently expanded in a finite series of non-orthogonal modes. Variational techniques are used to determine the time coefficients. Yasinsky (11) also used non-orthogonal modes in a time synthesis technique. The major disadvantage of the modal approach lies in the fact that a separation of variables is implemented and unless a perturbation is reasonably well tailored to the modes, a large number of modes may be required.

The most widely known numerical programs are the WIGLE

codes (12, 13) which provide the standard to which other techniques are compared. These codes utilize finite difference techniques and can handle non-linear feedback in a two-group analysis which may also include delayed neutrons.

Andrews and Hansen (14) assume that the neutron flux and precursor concentrations can be expressed as exponential functions between time steps. The second-order spatial derivative is approximated by the three-point central difference formula. The exponential time variation is not restricted to be the same at all space points. Their results compared favorably with WIGLE-40 in the cases considered and computer run times were also comparable.



### III. THEORETICAL DEVELOPMENT

#### A. Analytic Considerations

The space and time dependent multigroup diffusion equations in infinite slab geometry may be represented as

$$D_i^g \frac{\partial^2 \phi_i^g(x,t)}{\partial x^2} - \Sigma_i^g \phi_i^g(x,t) - V_g^{-1} \frac{\partial \phi_i^g(x,t)}{\partial t} + \sum_{g'=1}^N \chi_i^{g' \rightarrow g} \phi_i^{g'}(x,t) = f_i^g(x,t) \quad a_i \leq x \leq a_{i+1} \quad (1)$$

for the  $g^{\text{th}}$  group and  $i^{\text{th}}$  spacial region. The terms in Equation 1 are defined as:

- $\phi_i^g(x,t)$  = space and time dependent flux for energy group  $g$  in region  $i$ .
- $f_i^g(x,t)$  = space and time dependent external driving function.
- $D_i^g$  = diffusion coefficient.
- $\Sigma_i^g$  = cross section for removal of neutrons from  $g^{\text{th}}$  energy group by all processes.
- $V_g$  = neutron velocity associated with energy group  $g$ .
- $\chi_i^{g' \rightarrow g}$  = coupling coefficient for transference of  $g^{\text{th}}$  energy group neutrons to group  $g$  in region  $i$ . Includes both scattering and fission processes.

$N$  = total number of energy groups considered.

Unless otherwise specified, all terms without arguments may be taken as constants within a given energy group and spacial region.

Equation 1 is Laplace transformed and the resulting equation rearranged to obtain

$$\frac{d^2 \phi_i^g(x, s)}{dx^2} - (\alpha_i^g)^2 \phi_i^g(x, s) = \frac{1}{D_i^g} F_i^g(x, s) \quad , \quad (2)$$

where

$$\phi_i^g(x, s) = L\{\phi_i^g(x, t)\}$$

$$(\alpha_i^g)^2 = \mu_i^g \Sigma_i^g / D_i^g + \nu s v_g^{-1} / D_i^g \quad 0 \leq \mu_i^g \leq 1, \quad 0 \leq \nu \leq 1$$

$$F_i^g(x, s) = L\{f_i^g(x, t)\} + [(1 - \mu_i^g) \Sigma_i^g + (1 - \nu) s v_g^{-1}] \phi_i^g(x, t)$$

$$- \sum_{g'=1}^G \chi^{g'-g} \phi_i^{g'}(x, s) - v_g^{-1} \phi_i^g(x, t) \Big|_{+} = 0 \quad .$$

The terms  $\mu_i^g$  and  $\nu$  have been introduced for flexibility and are useful in the subsequent numerical treatment. For the purposes of this section it is sufficient to know that  $\mu_i^g$  will be greater than zero. If  $\nu$  is greater than zero,  $\alpha_i^g$  will be a function of  $s$ . To simplify the notation which follows,  $\nu$  is taken as zero.

A Green's function formulation will be utilized to represent an alternate integral form of Equation 2. This form is given for each energy group  $g$  and region  $i$  by

$$\phi_i^g(x, s) = \sum_{j=1}^I \int_{a_j}^{a_{j+1}} G_{ij}^g(x, \varepsilon) F_j^g(\varepsilon, s) d\varepsilon + A_i^g e^{\alpha_i^g x} + B_i^g e^{-\alpha_i^g x},$$

$$a_i \leq x \leq a_{i+1}, \quad a_j \leq \varepsilon \leq a_{j+1} \quad (3)$$

where  $G_{ij}^g(x, \varepsilon)$  is seen to represent the response at a point  $x$  in region  $i$  to a perturbation at point  $\varepsilon$  in region  $j$  and  $I$  is the total number of regions. It should be noted that had  $\nu$  been taken greater than zero,  $G_{ij}^g(x, \varepsilon)$  would be a function of  $s$  since it will be shown to depend on  $\alpha_i^g$ . The first term on the right hand side of Equation 3 represents the particular solution to Equation 2 while the second and third represent the homogeneous solution. It will be seen that for  $G_{ij}^g(x, \varepsilon)$  to exist,  $A_i^g = B_i^g = 0$  for all  $g$  and all  $i$ . This will be considered further at a later time but for the present the last two terms in Equation 3 as well as the group notation will be dropped. Thus for each energy group and each spacial region the proposed solution may be written as

$$\phi_i(x, s) = \sum_{j=1}^I \int_{a_j}^{a_{j+1}} G_{ij}(x, \varepsilon) F_j(\varepsilon, s) d\varepsilon.$$

$$a_i \leq x \leq a_{i+1}, \quad a_j \leq \varepsilon \leq a_{j+1} \quad (4)$$

To verify that Equation 4 represents the particular solution to Equation 2, Equation 4 must be differentiated twice with respect to  $x$ . The first yields

$$\begin{aligned} \frac{d\phi_i(x,s)}{dx} &= \sum_{\substack{j=1 \\ j \neq i}}^I \int_{a_j}^{a_{j+1}} \frac{dG_{ij}(x,\varepsilon)}{dx} F_j(\varepsilon,s) d\varepsilon \\ &+ \frac{d}{dx} \int_{a_i}^x G_{ii}^1(x,\varepsilon) F_i(\varepsilon,s) d\varepsilon \\ &+ \frac{d}{dx} \int_x^{a_{i+1}} G_{ii}^2(x,\varepsilon) F_i(\varepsilon,s) d\varepsilon \end{aligned}$$

where

$$G_{ii}(x,\varepsilon) = \left\{ \begin{array}{ll} G_{ii}^1(x,\varepsilon) & a_i \leq \varepsilon \leq x \leq a_{i+1} \\ G_{ii}^2(x,\varepsilon) & a_i \leq x \leq \varepsilon \leq a_{i+1} \end{array} \right\}. \quad (5)$$

$G_{ii}^2(x,\varepsilon)$  denotes the value of the Green's Function in region  $i$  for  $\varepsilon \geq x$  and does not denote the square of  $G_{ii}(x,\varepsilon)$ . Thus  $G_{ij}(x,\varepsilon)$  is continuous in  $x$  and  $\varepsilon$  in their respective regions when  $i \neq j$  but this constraint has not yet been placed on  $G_{ii}(x,\varepsilon)$  at the point  $x = \varepsilon$ . From Liebnitz' rule

for taking the derivative of an integral

$$\begin{aligned}
 \frac{d\phi_i(x,s)}{dx} &= \sum_{\substack{j=1 \\ j \neq i}}^I \int_{a_j}^{a_{j+1}} \frac{dG_{ij}(x,\varepsilon)}{dx} F_j(\varepsilon,s) d\varepsilon \\
 &+ \int_{a_i}^x \frac{dG_{ii}^1(x,\varepsilon)}{dx} F_i(\varepsilon,s) d\varepsilon \\
 &+ \int_x^{a_{i+1}} \frac{dG_{ii}^2(x,\varepsilon)}{dx} F_i(\varepsilon,s) d\varepsilon \\
 &+ [G_{ii}^1(x,\varepsilon) - G_{ii}^2(x,\varepsilon)]_{\varepsilon=x} F_i(x,s)
 \end{aligned}$$

where the continuity constraint on  $G_{ii}(x,\varepsilon)$  at the point  $x = \varepsilon$  eliminates the last term above. Again differentiating with respect to  $x$  yields

$$\begin{aligned}
 \frac{d^2\phi_i(x,s)}{dx^2} &= \sum_{\substack{j=1 \\ j \neq i}}^I \int_{a_j}^{a_{j+1}} \frac{d^2G_{ij}(x,\varepsilon)}{dx^2} F_j(\varepsilon,s) d\varepsilon \\
 &+ \int_{a_i}^x \frac{d^2G_{ii}^1(x,\varepsilon)}{dx^2} F_i(\varepsilon,s) d\varepsilon \\
 &+ \int_x^{a_{i+1}} \frac{d^2G_{ii}^2(x,\varepsilon)}{dx^2} F_i(\varepsilon,s) d\varepsilon +
 \end{aligned}$$

$$\left[ \frac{dG_{ii}^1(x, \varepsilon)}{dx} - \frac{dG_{ii}^2(x, \varepsilon)}{dx} \right]_{\varepsilon=x} F_i(x, s) \quad . \quad (6)$$

Substituting Equations 4 and 6 into Equation 2 and rearranging yields

$$\begin{aligned} & \sum_{\substack{j=1 \\ j \neq i}}^I \int_{a_j}^{a_{j+1}} \left[ \frac{d^2 G_{ij}(x, \varepsilon)}{dx^2} - \alpha_i^2 G_{ij}(x, \varepsilon) \right] F_j(\varepsilon, s) d\varepsilon \\ & + \int_{a_i}^x \left[ \frac{d^2 G_{ii}^1(x, \varepsilon)}{dx^2} - \alpha_i^2 G_{ii}^1(x, \varepsilon) \right] F_i(\varepsilon, s) d\varepsilon \\ & + \int_x^{a_{i+1}} \left[ \frac{d^2 G_{ii}^2(x, \varepsilon)}{dx^2} - \alpha_i^2 G_{ii}^2(x, \varepsilon) \right] F_i(\varepsilon, s) d\varepsilon \\ & + \left[ \frac{dG_{ii}^1(x, \varepsilon)}{dx} - \frac{dG_{ii}^2(x, \varepsilon)}{dx} \right]_{\varepsilon=x} F_i(x, s) \\ & = F_i(x, s) / D_i \quad . \quad (7) \end{aligned}$$

Thus if the  $G_{ij}(x, \varepsilon)$  are constructed to satisfy the following equations

$$\frac{d^2 G_{ij}(x, \varepsilon)}{dx^2} - \alpha_i^2 G_{ij}(x, \varepsilon) = 0 \quad a_i \leq x \leq a_{i+1}, \quad a_j \leq \varepsilon \leq a_{j+1}, \quad i \neq j$$

$$\frac{d^2 G_{ii}^1(x, \varepsilon)}{dx^2} - \alpha_i^2 G_{ii}^1(x, \varepsilon) = 0 \quad a_i \leq \varepsilon \leq x \leq a_{i+1}$$

$$\frac{d^2 G_{ii}^2(x, \varepsilon)}{dx^2} - \alpha_i^2 G_{ii}^2(x, \varepsilon) = 0 \quad a_i \leq x \leq \varepsilon \leq a_{i+1}$$

$$G_{ii}^1(x, \varepsilon) \Big|_{\varepsilon=x} - G_{ii}^2(x, \varepsilon) \Big|_{\varepsilon=x} = 0$$

$$\left[ \frac{dG_{ii}^1(x, \varepsilon)}{dx} - \frac{dG_{ii}^2(x, \varepsilon)}{dx} \right]_{\varepsilon=x} = 1/D_i$$

then Equation 4 represents an alternate integral formulation of Equation 2. The general solutions to these equations are given by

$$G_{ij}(x, \varepsilon) = A_{ij}(\varepsilon) e^{\alpha_i x} + B_{ij}(\varepsilon) e^{-\alpha_i x} \quad i \neq j, \quad a_i \leq x \leq a_{i+1},$$

$$a_j \leq \varepsilon \leq a_{j+1} \quad (8a)$$

$$G_{ii}^1(x, \varepsilon) = A_{ii}(\varepsilon) e^{\alpha_i x} + B_{ii}(\varepsilon) e^{-\alpha_i x} \quad a_i \leq \varepsilon \leq x \leq a_{i+1} \quad (8b)$$

$$G_{ii}^2(x, \varepsilon) = A_{ii}(\varepsilon) e^{\alpha_i x} + B_{ii}(\varepsilon) e^{-\alpha_i x} + \frac{1}{\alpha_i D_i} \sinh \alpha_i (\varepsilon - x)$$

$$a_i \leq x \leq \varepsilon \leq a_{i+1} \quad (8c)$$

For I spacial regions, Equations 8a,b,c present 2I unknowns

(i.e.  $A_{ij}(\epsilon)_1 B_{ij}(\epsilon)$   $j=1.2\dots I$ ). It should be noted that one such set will exist for each spacial region  $i$  in each energy group  $g$ . These  $2I$  unknowns must be determined so as to satisfy the boundary conditions and, if  $I > 1$ , interface conditions given by

$$\phi_1(a_1, s) = 0 \quad (9a)$$

$$\phi_I(a_{I+1}, s) = 0 \quad (9b)$$

$$\phi_i(a_{i+1}, s) = \phi_{i+1}(a_{i+1}, s) \quad (9c)$$

$$D_i \frac{d\phi_i(a_{i+1}, s)}{dx} = D_{i+1} \frac{d\phi_{i+1}(a_{i+1}, s)}{dx} \quad (9d)$$

Applying these conditions to Equations 8a, 8b, 8c and writing the resulting set of equations in matrix form yields

$$C A(\epsilon) = E(\epsilon) \quad (10a)$$

and hence

$$A(\epsilon) = C^{-1} E(\epsilon) \quad . \quad |C| \neq 0 \quad (10b)$$

The matrices  $A(\epsilon)$ ,  $C$ , and  $E(\epsilon)$  are given for  $I = 3$  by

$$A(\epsilon) = \begin{bmatrix} A_{11}(\epsilon) & A_{12}(\epsilon) & A_{13}(\epsilon) \\ B_{11}(\epsilon) & B_{12}(\epsilon) & B_{13}(\epsilon) \\ A_{21}(\epsilon) & A_{22}(\epsilon) & A_{23}(\epsilon) \\ B_{21}(\epsilon) & B_{22}(\epsilon) & B_{23}(\epsilon) \\ A_{31}(\epsilon) & B_{32}(\epsilon) & B_{33}(\epsilon) \\ B_{31}(\epsilon) & B_{32}(\epsilon) & B_{33}(\epsilon) \end{bmatrix} \quad .$$



$$C = \begin{bmatrix} e^{\alpha_1 a_1} & -e^{-\alpha_1 a_1} & 0 & 0 & 0 & 0 \\ e^{\alpha_1 a_2} & -e^{-\alpha_1 a_2} & -e^{\alpha_2 a_2} & -e^{-\alpha_2 a_2} & 0 & 0 \\ \gamma_1 e^{\alpha_1 a_2} & -\gamma_1 e^{-\alpha_1 a_2} & -\gamma_2 e^{\alpha_2 a_2} & +\gamma_2 e^{-\alpha_2 a_2} & 0 & 0 \\ 0 & 0 & e^{\alpha_2 a_3} & -e^{-\alpha_2 a_3} & -e^{\alpha_3 a_3} & -e^{-\alpha_3 a_3} \\ 0 & 0 & \gamma_2 e^{\alpha_2 a_3} & -\gamma_2 e^{-\alpha_2 a_3} & -\gamma_3 e^{\alpha_3 a_3} & +\gamma_4 e^{-\alpha_3 a_3} \\ 0 & 0 & 0 & 0 & e^{\alpha_3 a_4} & -e^{-\alpha_3 a_4} \end{bmatrix}$$

where  $\gamma_i = \alpha_i D_i$ , and by

$$E(\varepsilon) = \begin{bmatrix} \frac{1}{\alpha_1 D_1} \sinh \alpha_1 (\varepsilon - a_1) & 0 & 0 \\ 0 & \frac{1}{\alpha_2 D_2} \sinh \alpha_2 (\varepsilon - a_2) & 0 \\ 0 & -\cosh \alpha_2 (\varepsilon - a_2) & 0 \\ 0 & 0 & \frac{1}{\alpha_3 D_3} \sinh \alpha_3 (\varepsilon - a_3) \\ 0 & 0 & -\cosh \alpha_3 (\varepsilon - a_3) \\ 0 & 0 & 0 \end{bmatrix}$$

Since  $C$  and  $E(\varepsilon)$  represent known quantities,  $A(\varepsilon)$  and hence the various  $G_{ij}(x, \varepsilon)$  can be determined providing  $|C| \neq 0$ . If  $|C| = 0$  then  $G_{ij}(x, \varepsilon)$  does not exist. This brings up the question of the homogeneous part of Equation 3. If a homogeneous solution exists it must satisfy the matrix equation

$$C\bar{y} = 0 \quad (11)$$

where  $C$  is the same as above and  $\bar{y}$  is given for  $I = 3$  by

$$\bar{y} = \begin{bmatrix} A_1 \\ B_1 \\ A_2 \\ B_2 \\ A_3 \\ B_3 \end{bmatrix} .$$

Thus for a non-zero homogeneous solution, the determinant of  $C$  must vanish. Therefore a condition for the use of this approach, namely that  $|C| \neq 0$ , precludes a non-zero homogeneous solution.

Defining the overall Green's Function matrix  $G(x, \varepsilon)$  for  $I = 3$  to be

$$G(x, \varepsilon) = \begin{bmatrix} G_{11}(x, \varepsilon) & G_{12}(x, \varepsilon) & G_{13}(x, \varepsilon) \\ G_{21}(x, \varepsilon) & G_{22}(x, \varepsilon) & G_{23}(x, \varepsilon) \\ G_{31}(x, \varepsilon) & G_{32}(x, \varepsilon) & G_{33}(x, \varepsilon) \end{bmatrix} , \quad (12)$$

then  $G(x, \varepsilon)$  may be obtained by

$$G(x, \varepsilon) = B(x)A(\varepsilon) + D(x, \varepsilon) \quad (13)$$

where for  $I = 3$

$$B(x) = \begin{bmatrix} e^{\alpha_1 x} & e^{-\alpha_1 x} & 0 & 0 & 0 & 0 \\ 0 & 0 & e^{\alpha_2 x} & e^{-\alpha_2 x} & 0 & 0 \\ 0 & 0 & 0 & 0 & e^{\alpha_3 x} & e^{-\alpha_3 x} \end{bmatrix}$$

and  $D(x, \varepsilon)$  is defined by

$$D(x, \varepsilon) = \text{DIAG} \left[ \frac{U(\varepsilon-x)}{\alpha_1 D_1} \sinh \alpha_1 (\varepsilon-x), \frac{U(\varepsilon-x)}{\alpha_2 D_2} \sinh \alpha_2 (\varepsilon-x), \frac{U(\varepsilon-x)}{\alpha_3 S_3} \sinh \alpha_3 (\varepsilon-x) \right] .$$

Substituting Equation 10b into Equation 13 yields

$$G(x, \varepsilon) = B(x)C^{-1}E(\varepsilon) + D(x, \varepsilon) \quad (14)$$

The elements of the matrix  $G(x, \varepsilon)$  correspond to the desired  $G_{ij}(x, \varepsilon)$  in Equation 4 since

$$G(x, \varepsilon) = G_{ij}(x, \varepsilon) \quad a_i \leq x \leq a_{i+1}, \quad a_j \leq \varepsilon \leq a_{j+1} \quad (15)$$

Defining

$$\int_x h(\varepsilon) d\varepsilon$$

to be the integral of  $h(\varepsilon)$  over its region of definition in  $x$  space, and restoring the energy group notation,

$$\bar{\phi}^g(x, s) = \int_x G^g(x, \epsilon) \bar{F}^g(\epsilon, s) d\epsilon \quad (16)$$

represents the set of equations given by Equation 15 with  $i = 1, 2, \dots, I$ . Thus  $\bar{\phi}^g(x, s)$  and  $\bar{F}^g(\epsilon, s)$  are defined as

$$\bar{\phi}^g(x, s) = \begin{bmatrix} \phi_1^g(x, s) \\ \phi_2^g(x, s) \\ \vdots \\ \phi_I^g(x, s) \end{bmatrix}$$

and

$$\bar{F}^g(\epsilon, s) = \begin{bmatrix} F_1^g(\epsilon, s) \\ F_2^g(\epsilon, s) \\ \vdots \\ F_I^g(\epsilon, s) \end{bmatrix} .$$

For  $N$  energy groups, there will be  $N$  equations like Equation 16. This set represents an implicit integral formulation since  $\bar{F}^g(x, s)$  contains coupling terms from other groups. To demonstrate this and provide a basis for the energy group matrix structure which follows,  $\bar{F}^g(x, s)$  is broken into its components

$$\bar{F}^g(x, s) = \Omega^g \bar{\varphi}^g(x, s) - \sum_{g'=1}^N \chi^{g'+g} \bar{\varphi}^{g'}(x, s) - v_g^{-1} \bar{\varphi}^g(x, t) \Big|_{t=0}$$

where

$$\chi^{g'+g} = \text{DIAG}[\chi_1^{g'+g}, \chi_2^{g'+g}, \dots, \chi_I^{g'+g}]$$

and

$$\Omega^g = \text{DIAG}[(1-\mu_1^g) \Sigma_1^g + (1-\nu) s v_g^{-1}, \dots, (1-\mu_I^g) \Sigma_I^g + (1-\nu) s v_g^{-1}]$$

Equation 16 now becomes for each group  $g$

$$\begin{aligned} \bar{\varphi}^g(x, s) = & \int_x G^g(x, \varepsilon) \Omega^g \bar{\varphi}^g(\varepsilon, s) d\varepsilon - \sum_{g'=1}^n \int_x G^g(x, \varepsilon) \chi^{g'+g} \bar{\varphi}^{g'}(\varepsilon, s) d\varepsilon \\ & - v_g^{-1} \int_x G^g(x, \varepsilon) \bar{\varphi}^g(\varepsilon, t) \Big|_{t=0} d\varepsilon \end{aligned} \quad (17)$$

which may be written in matrix-operator form as

$$\bar{\varphi}(x, s) = GF\bar{\varphi}(x, s) - \bar{y}(x) \quad (18)$$

where

$$\bar{\varphi}(x, s) = \begin{bmatrix} \bar{\varphi}^1(x, s) \\ \bar{\varphi}^2(x, s) \\ \vdots \\ \bar{\varphi}^N(x, s) \end{bmatrix},$$

$$\bar{y}(x) = \begin{bmatrix} V_1^{-1} \int_x G^1(x, \varepsilon) \varphi^1(\varepsilon, t) \Big|_{t=0} d\varepsilon \\ \vdots \\ V_N^{-1} \int_x G^N(x, \varepsilon) \varphi^1(\varepsilon, t) \Big|_{t=0} d\varepsilon \end{bmatrix} \quad (19)$$

and the matrix of operators GF is defined by

$$GF = \begin{bmatrix} GF_{11} & GF_{12} & \dots & GF_{1N} \\ GF_{21} & GF_{22} & & \cdot \\ \cdot & & & \cdot \\ \cdot & & & \cdot \\ GF_{N1} & \cdot & \cdot & \cdot & \cdot & GF_{NN} \end{bmatrix}$$

where the operation  $GF_{gg'} \bar{\varphi}^{g'}(x, s)$  is defined by

$$GF_{gg'} \bar{\varphi}^{g'}(x, s) = - \int_x G^g(x, \varepsilon) [X^{g' \rightarrow g} - \delta_{g', g} \Omega^g] \bar{\varphi}^{g'}(\varepsilon, s) d\varepsilon$$

and

$$\begin{aligned} \delta_{g'g} &= 0 \quad g' \neq g \\ &= 1 \quad g' = g \end{aligned}$$

Solving Equation 17 for  $\bar{\varphi}(x, s)$  yields

$$\bar{\varphi}(x, s) = [I - GF]^{-1} \bar{y}(x) \quad (20)$$

Equation 20 is not particularly useful from an analytic view

point but is useful numerically. The integrals involved may be approximated numerically to yield a form exactly like that of Equation 20.

### B. Numerical Considerations

The integrals arising from the Green's function formulation pose an unusual problem. The problem originates with the discontinuous first derivative of  $G(x, \varepsilon)$  at  $\varepsilon = x$ . Consider Equation 21, a special case of Equation 4, which represents the flux in region one from a two region model.

$$\phi_1(x, \varepsilon) = \int_{a_1}^{a_2} G_{11}(x, \varepsilon) F_1(\varepsilon, s) d\varepsilon + \int_{a_2}^{a_3} G_{12}(x, \varepsilon) F_2(\varepsilon, s) d\varepsilon \quad (21)$$

to perform the integration, the first integral must be divided into two parts at the point  $\varepsilon = x$  yielding

$$\begin{aligned} \phi_1(x, \varepsilon) = & \int_{a_1}^x G_{11}^1(x, \varepsilon) F_1(\varepsilon, s) d\varepsilon + \int_x^{a_2} G_{11}^2(x, \varepsilon) F_1(\varepsilon, s) d\varepsilon \\ & + \int_{a_2}^{a_3} G_{12}(x, \varepsilon) F_2(\varepsilon, s) d\varepsilon \quad . \end{aligned} \quad (22)$$

Consider an arbitrary grid in which equal spacing exists within a region but the spacing may vary from region to region. Let  $x_1 = a_1$ ,  $x_{N1} = a_2$ ,  $x_{N2} = a_3$ . Approximate

Equation 22 by

$$\begin{aligned}
 \phi_1(x_n, s) = & \sum_{i=1}^n w_i G_{11}^1(x_n, x_i) F_1(x_i, s) \Delta_1 \\
 & + \sum_{i=n}^{N1} w_i G_{11}^2(x_n, x_i) F_1(x_i, s) \Delta_1 \\
 & + \sum_{i=N1}^{N2} w_i G_{12}(x_n, x_i) F_2(x_i, s) \Delta_2 \quad (23a)
 \end{aligned}$$

where  $\Delta_j$  = grid spacing interval in region  $j$ . The  $w_i$  depend on the number of terms in each summation as well as the index  $i$ . It should be noted that there is an overlap of indexing between successive summations. This does not imply that weights with the same index are equal. It does imply that the last term of the preceding summation plus the first term of the following summation make up the contribution to  $\phi_1(x_n, s)$  from  $F(x, s)$  in the area near  $x_i$ . Figure 1 illustrates this nicely. For  $\phi_1(x_2, s)$  the  $w_1$  and  $w_2$  from the first summation in Equation 23a are the first order (trapezoid rule) weights and  $w_2, w_3, w_4$  and  $w_5$  from the second summation are the third order weights. For  $\phi_1(x_3, s)$  both summations would utilize second order weights. The third summation would use fourth order weighting for  $x_n = x_1, x_2, \dots, x_5$ . For  $x_n = x_6, \dots, x_9$ , the second summation would be divided at  $x_i = x_n$  and the first would span the first region thereby using fourth order weights. Thus the order of



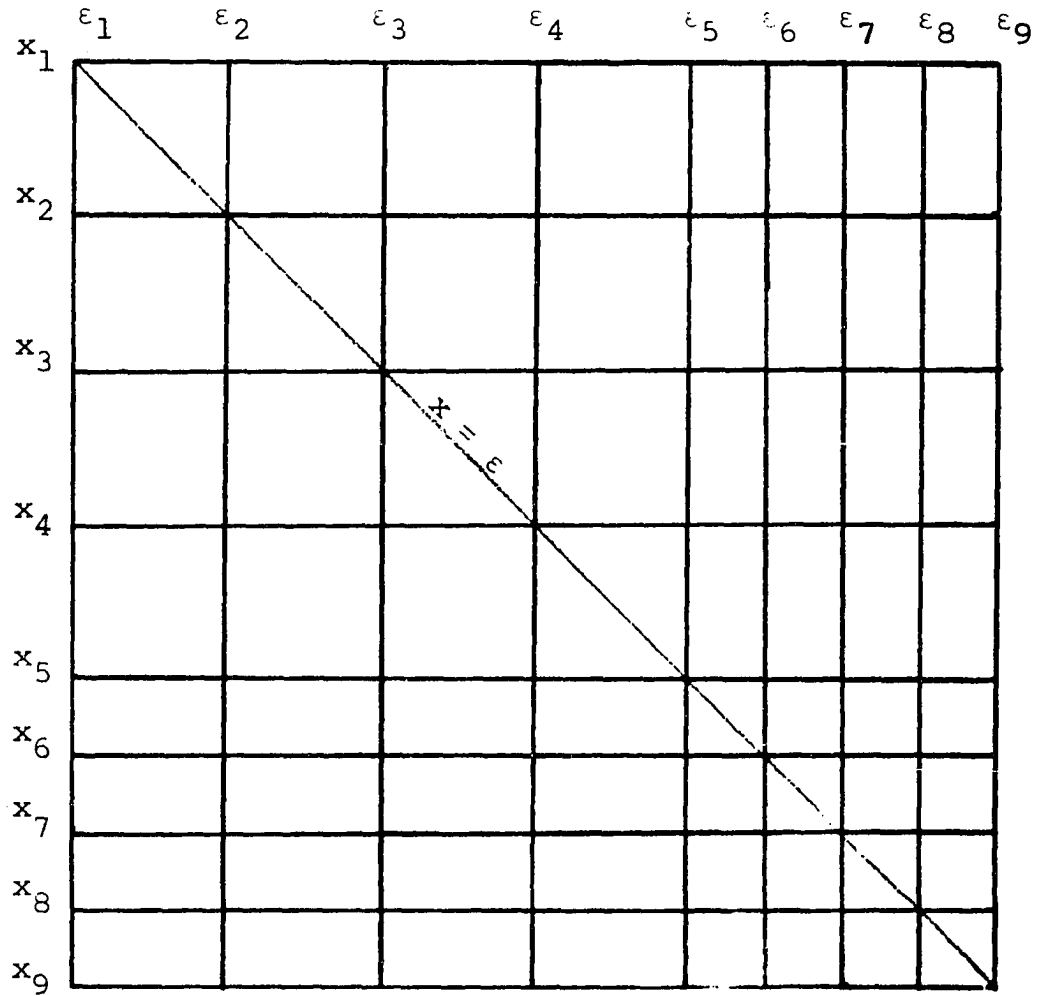


Figure 1. Sample grid for two region with interface at  $x_{N1} = x_5$

approximation of the integrals in Equation 21 is a function of the location of the discontinuity. As a consequence, the flux determination for a point near a boundary is less accurate than those further from the boundary. Fortunately the effect of this can be checked by simply varying the grid size and comparing the resulting flux profiles near the boundary.

In Equation 23a some of the notation is unnecessary. Since the Green's function is continuous, the subscripts denoting the region of  $x_n$  and  $x_i$  may be dropped. The superscript denoting which functional representation to use when  $x_i$  and  $x_n$  are in the same region may also be dropped as the relative sizes of  $x_i$  and  $x_n$  determine this. The region notation on the driving function and the spacing interval must be retained as they are not, in general, continuous at the interface. Equation 23a may thus be rewritten as

$$\begin{aligned} \phi(x_n, s) = & \sum_{i=1}^n w_i G(x_n, x_i) F_1(x_i, s) \Delta_1 + \sum_{i=n}^{N1} w_i G(x_n, x_i) F_1(x_i, s) \Delta_1 \\ & + \sum_{i=N1}^{N2} w_i G(x_n, x_i) F_2(x_i, s) \Delta_2 \end{aligned} \quad (23b)$$

$$a_1 \leq x_n \leq a_2 \quad ,$$

and the expression for the flux in region two is

$$\begin{aligned} \phi(x_n, s) = & \sum_{i=1}^{N1} w_i G(x_n, x_i) F_1(x_i, s) \Delta_1 + \sum_{i=N1}^n w_i G(x_n, x_i) F_2(x_i, s) \Delta_2 \\ & + \sum_{i=n}^{N2} w_i G(x_n, x_i) F_2(x_i, s) \Delta_2 \end{aligned} \quad (23c)$$

$$a_2 \leq x_n \leq a_3 \quad .$$

In general for  $N$  regions there will be  $N$  expressions containing  $N + 1$  summations since two summations are necessary when  $x_n$  and  $x_i$  are in the same region. It is convenient at this point to consider the group dependence before proceeding.  $\phi(x_n, s)$ ,  $G(x_n, x_i)$  and  $F_j(x_i, s)$  should be replaced by  $\phi^g(x_n, s)$ ,  $G^g(x_n, x_i)$  and  $F_j^g(x_i, s)$ . Further  $F_j^g(x_i, s)$  is, in general, made up of linear combinations of all group fluxes as well as the initial flux for that particular group.  $F_j^g(x_i, s)$  may also contain an external source term which could be  $s$  dependent. This would, however, be handled in the same manner as the initial flux for group  $g$  and need not be considered separately. It would become part of  $\bar{y}$  which would be  $s$  dependent if the external source term were.

For the two region example, there would be  $G$  sets of equations like Equations 23b,c for  $G$  energy groups. For the more general case of  $G$  groups and  $N$  regions, there would be  $G \times N$  equations each containing  $N + 1$  summation terms.

It is convenient to seek a more compact form for

Equations 23b,c for each group  $g$ . This form is given for the two region case by

$$\phi^g(x_n, s) = \sum_{i=1}^{N2} W_{nk} G^g(x_n, x_i) F^g(x_i, s) \quad (24a)$$

where  $G^g(x_n, x_i)$  is the same as in Equations 23b,c but the remaining terms require careful attention. The difficulty arises from the overlapping  $w_i$  between adjacent summations in Equations 23b,c and from the lack of continuity of  $F^g(x_i, s)$  at the interface between the two regions.  $F^g(x_i, s)$  is defined by

$$F^g(x_i, s) = \begin{cases} F_1^g(x_i, s) \Delta_1 & x_i < x_{N1} \\ F_2^g(x_i, s) \Delta_2 & x_i > x_{N1} \end{cases} \quad (24b)$$

and for the present remains undefined at the interface  $x_i = x_{n1}$ .  $W_{ni}$  is defined as

$$W_{ni} = w_i \quad i \neq n, N1$$

and is yet to be defined at  $i = n$  and  $i = N1$ . In the general case of  $N$  regions  $F^g(x_i, s)$  and  $W_{ni}$  would be undefined at the  $N-1$  interfaces and  $W_{ni}$  would be undefined at  $i = n$ . Complicating the definition of  $W_{nn}$  is the fact that it may be in either region of the two region case. Referring to Equations 23b,c and the two region case

$$W_{nn} = w_n^1 + w_n^2 \quad n \neq N1 \quad (24c)$$

where

$$w_n^1 = w_n \quad \text{from summation for which } i \leq n$$

$$w_n^2 = w_n \quad \text{from summation for which } i \geq n$$

irrespective of the region to which  $n$  refers.  $W_{nN1}$  and  $F^g(x_{N1}, s)$  cannot be defined separately but must be defined as a product.

$$W_{nN1} F^g(x_{N1}, s) = w_{N1}^1 F_1^g(x_{N1}, s) \Delta_1 + w_{N1}^2 F_2^g(x_{N1}, s) \Delta_2 \quad (24d)$$

where

$$w_{N1}^1 = W_{N1} \quad \text{from summation for which } i \leq N1$$

$$w_{N1}^2 = W_{N1} \quad \text{from summation for which } i \geq N1$$

and  $F_1^g(x_{N1}, s)$  and  $F_2^g(x_{N1}, s)$  are defined as they were for Equations 23a,b. For the more general case of  $N$  regions there will be  $N-1$  equations of the form of Equation 24d for the additional interfaces. Equations 24a,b,c must be amended accordingly. In Equation 24a,  $N2$  would be replaced by  $N$ .

Equation 24a provides the basis from which a final form like Equation 20 is encountered.  $F^g(x_i, s)$  must first be broken into its components. To better illustrate the

procedure, a two energy group, multi-region model will be assumed. The Laplace transformed two group equations are given for each region  $i$  by

$$D_i^1 \frac{d^2 \phi_i^1(x, s)}{dx^2} - \Sigma_i^1 \phi_i^1(x, s) = sV_1^{-1} \phi_i^1(x, s) - (v\Sigma_f)_i^2 \phi_i^2(x, s) - v_1^{-1} \phi_i^1(x, t) \Big|_{t=0} \quad (25a)$$

$$D_i^2 \frac{d^2 \phi_i^2(x, s)}{dx^2} - \Sigma_i^2 \phi_i^2(x, s) = -\Sigma_i^1 \phi_i^1(x, s) + (sV_2^{-1} + \delta\Sigma_i^2) \phi_i^2(x, s) - v_2^{-1} \phi_i^2(x, t) \Big|_{t=0} \quad (25b)$$

where only thermal group fissions are considered with all fission neutrons entering the fast group. The absorption cross section for fast neutrons is considered negligible and all neutrons removed from the fast group enter the thermal group. The system is assumed initially critical prior to a step perturbation in the thermal cross section at  $t = 0$ . The quantities on the right hand sides of Equations 25a,b are  $F_i^1(x, s)$  and  $F_i^2(x, s)$  respectively.

From Equation 24a, Equations 25a,b become

$$\begin{aligned} \phi^1(x_n, s) = & \sum_{i=1}^I W_{ni} G^1(x_n, x_i) [s v_1^{-1} \phi^1(x_i, s) - (v \Sigma_f)_i^2 \phi^2(x_i, s) \\ & - v_1^{-1} \phi_i^1(x_i, t) \Big|_{t=0} ] \end{aligned} \quad (26a)$$

$$\begin{aligned} \phi^2(x_n, s) = & \sum_{i=1}^I W_{ni} G^2(x_n, x_i) [-\Sigma_i^1 \phi^1(x_i, s) + (x v_2^{-1} + \delta \Sigma_i^2) \phi^2(x_i, s) \\ & - v_2^{-1} \phi_i^2(x_i, t) \Big|_{t=0} ] \end{aligned} \quad (26b)$$

where the subscript  $i$  now denotes the grid position and  $I-2$  is the total number of interior mesh points. This set of equations can be written in matrix form as

$$\begin{aligned} \begin{bmatrix} \bar{\phi}^1(s) \\ \bar{\phi}^2(s) \end{bmatrix} &= \begin{bmatrix} GF^{11}(s) & GF^{12}(s) \\ GF^{21}(s) & GF^{22}(s) \end{bmatrix} \begin{bmatrix} \bar{\phi}^1(s) \\ \bar{\phi}^2(s) \end{bmatrix} + \begin{bmatrix} \bar{y}^1 \\ \bar{y}^2 \end{bmatrix} \end{aligned} \quad (27a)$$

where

$$\bar{\phi}^g(s) = \begin{bmatrix} \phi^g(x_1, s) \\ \vdots \\ \phi^g(x_{N2}, s) \end{bmatrix}$$

$$\bar{y}^g = \begin{bmatrix} - \sum_{i=1}^{N2} W_{1i} G^g(x_1, x_i) V_g^{-1} \phi^g(x_i, t) \Big|_{t=0} \\ \vdots \\ - \sum_{i=1}^{N2} W_{N2i} G^g(x_{N2}, x_i) V_g^{-1} \phi^g(x_i, t) \Big|_{t=0} \end{bmatrix} \quad (27b)$$

and  $GF^{gg'}$  is a matrix each element of which is given by

$$GF_{ni}^{gg'} = W_{ni} G^g(x_n, x_i) f_i^{g'}(s)$$

where  $f_i^{g'}(s)$  represents terms such as  $-(v\Sigma_f)_i^2$ ,  $-\Sigma_i^1$ ,  $sV_1^{-1}$  and  $(sV_2^{-1} + \delta\Sigma_i^2)$  from Equations 26a,b.

Equation 27 may now be written in the same form as Equation 20.

$$\bar{\phi}(s) = [I - GF(s)]^{-1} \bar{y} \quad (28)$$

The important difference is that this is an explicit equation allowing  $\bar{\phi}(s)$  to be determined numerically. This formulation can easily be extended for any number of energy groups, space regions and space points. The practical limitations are brought about by such considerations as storage space in the computer and the expense associated with carrying out the inversion of  $[I - GF(s)]$ . An important consideration is the fact that the matrix  $[I - GF(s)]^{-1}$  is independent of  $\bar{y}$  and hence a wide range of  $\bar{y}$  could be considered



if this matrix is saved. It is important to realize that perturbations must occur across an entire region and thus the regions should be carefully chosen in generating this matrix. A time dependent external source can be utilized so long as this time dependence may be handled by the Laplace transform.

### C. Numerical Inversion

The ultimate worth of a solution to a partial differential equation in the Laplace transform domain is determined by the ability to obtain the time domain solution from it. One of the stated goals of this thesis was to determine whether an inversion technique presented in a text by Bellman et al. (1) would perform the task in this case. The method, which will be outlined, is one of a number suggested in this text and appeared particularly suitable as it utilizes a polynomial in  $e^{-t/\alpha}$  to approximate the time behavior. Since the diffusion equation is first order in time, one might expect approximately exponential behavior for step perturbations in a system with otherwise time stationary parameters.

The Laplace transform of  $u(t)$  is given by

$$F(s) = L\{u(t)\} = \int_0^{\infty} e^{-st} u(t) dt \quad ,$$

which may be written as

$$F(P/\alpha) = \int_0^{\infty} e^{-\frac{Pt}{\alpha}} u(t) dt \quad , \quad (29)$$

with  $p = \alpha s$ .

Defining the change of variables  $r = e^{-t/\alpha}$  and dividing by  $\alpha$ , Equation 29 becomes

$$\frac{F(P/\alpha)}{\alpha} = \int_0^1 r^{P-1} u(-\alpha \ln r) dr \quad . \quad (30)$$

Making the assumption that  $u(-\alpha \ln r)$  may be well approximated in the mean square sense by a polynomial in  $r$ , i.e. that  $u(t)$  is well represented as a finite series in

$$a_n e^{-\frac{n}{\alpha} t} \quad ,$$

leads directly to the use of a Gaussian quadrature to represent this integral. The Gaussian quadrature for  $N$  points gives the same accuracy as the more elementary quadratures would for  $2N$  points. That is to say that with  $N$  points it approximates the integrand as a polynomial of order  $2N-1$  as would the more elementary quadratures with  $2N$  points. This increased accuracy is paid for through the loss of freedom to specify the points or discrete times at which  $u(t)$  is to be determined. Equation 30 is thus represented by the approximation

$$\frac{F(P/\alpha)}{\alpha} \approx \sum_{i=1}^N w_i r_i^{P-1} u(-\alpha \ln r_i) \quad P = 1, 2, \dots, N \quad (31)$$

where  $t_i = -\alpha \ln r_i$  and  $r_i$  are the roots of the polynomial  $P_N(r)$ . This may be solved for  $u(-\alpha \ln r_i)$  and rewritten in matrix form as

$$\bar{u} = A^{-1} \bar{F} \quad (32)$$

where

$$\bar{u} = \begin{bmatrix} u(-\alpha \ln r_1) \\ \vdots \\ u(-\alpha \ln r_N) \end{bmatrix}$$

and

$$\bar{F} = \frac{1}{\alpha} \begin{bmatrix} F\left(\frac{1}{\alpha}\right) \\ \vdots \\ F\left(\frac{N}{\alpha}\right) \end{bmatrix}$$

and the  $i^{\text{th}}$  row and the  $j^{\text{th}}$  column of  $A$  is given by

$$A_{ij} = w_i r_i^{j-1}$$

Reference 1 specifies the elements of  $A^{-1}$ , the roots  $r_i$ , and  $-\ln r_i$  for  $N = 3$  through  $N = 15$ .

As a rule one wishes to obtain the inversions for as

large an  $N$  as possible to obtain the best approximation. The problem is not as simple as that in this case. The matrix  $A$  is ill conditioned in the sense that  $A^{-1}$  contains elements of both sign which are large in magnitude. This condition worsens as  $N$  increases and causes large changes in  $u(t)$  for correspondingly small changes in  $F(s)$ . This means that for large  $N$ , an accurate determination of  $F(s)$  is necessary to obtain  $u(t)$ . If one has accuracy to four significant figures for  $F(s)$  and a change in the fifth significant figure of  $F(s)$  produces a change in the first significant figure of  $u(t)$ , one can attach little meaning to the values of  $u(t)$  obtained. The number of significant figures obtainable in  $\bar{\vartheta}(s)$  will thus be an important factor.

Some comments in reference 1 are pertinent in defining the limitations of the inversion which become limitations of this method. It points out that the method cannot be expected to handle high frequency oscillations in time behavior. If success is to be expected  $u(t)$  must be a reasonably smooth function of time. This is not seen to be a severe limitation in the case at hand but should serve as a warning not to expect good results from, for instance, a high frequency cosine external source input.

## IV. APPLICATION AND MODEL USED

The reactor model chosen to test the formulation in a two group configuration is shown in Figure 2.

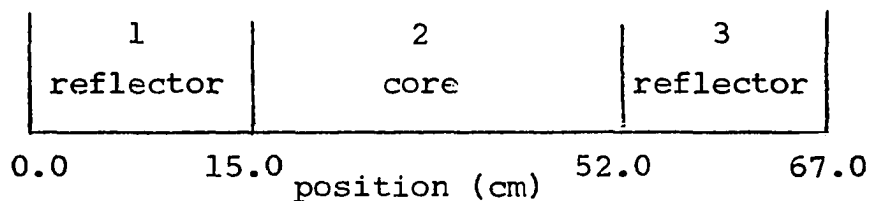


Figure 2. Reactor model

The steady state initial parameters are given in Table 1. The model is a slab representation of a light water moderated and reflected reactor with enriched uranium fuel. As may be seen in Table 1, the fast neutron absorption cross section is taken to be zero and all fissions are assumed to occur in the thermal group with the fission neutrons entering the fast group. This model was used previously by Loewe (15) and later by McFadden (10). The original intention was to consider the same perturbations as the latter and compare results along with those obtained from WIGLE-40. A problem arose, however, due to the fact that the perturbations he considered were given in terms of percent reactivity insertion rather than the magnitude of cross section change. As this parameter is given as an output from WIGLE-40, considerable time and expense might be expended in determining the

Table 1. Steady state initial parameters

Parameter	Units	Core	Reflector
$v_f^{-1}$	sec/cm	$3.50(10^{-7})$	$3.50(10^{-7})$
$v_s^{-1}$	sec/cm	$4.55(10^{-6})$	$4.55(10^{-6})$
$D_f$	cm	1.24	1.14
$D_s$	cm	0.26	0.16
$\Sigma_{r1}$	$\text{cm}^{-1}$	0.0207	0.0346
$p$	---	1.0	1.0
$\Sigma_{a1}$	$\text{cm}^{-1}$	0.0	0.0
$\Sigma_{r2}$	$\text{cm}^{-1}$	0.0817	0.0118
$v\Sigma_f$	$\frac{\text{neutrons}}{\text{fission-cm}}$	0.0985	0.0

appropriate cross section change which would produce this same reactivity change. Thus WIGLE-40 will serve as the basis for comparison in the problems considered.

The model is especially useful since the unperturbed state is symmetric about the center. Choosing a symmetric space grid thus constrains the Green's function to be sym-

metric. Since the symmetry is not used in the formulation, it provides a good check of the Green's function generated. In the symmetric problem the following relation must exist:

$$G(x, \varepsilon) = G(\varepsilon, x) = G(67.0-x, 67.0-\varepsilon) = G(67.0-\varepsilon, 67.0-x) \quad .$$

The Green's functions for problem one exhibit this.

One must decide upon the space dependence of the perturbation before setting up the Green's function. This is a direct consequence of the desire to avoid integrating across a discontinuity in either a system property or an external driving function. Thus if one wishes to perturb only a part of one of the regions in the model considered, this part should be made into a region itself. In the problems which follow there will be no external source considered. If one were to be considered it would become part of  $\bar{y}$  and if the external driving function were time dependent,  $\bar{y}$  would be a function of  $s$ . The concept of an external source as considered here refers to a space and time dependent source of neutrons which is not a function of the flux level. It does not allow a current source at a boundary for example. Such a source would change the original boundary conditions which would in turn change the Green's function. This could have been incorporated but as this study is an examination of the feasibility of the general approach it was not considered.

Problem one considers uniform perturbations of  $\Sigma_2^2$  in the second region of the reactor model. Thus a symmetric

space grid may be utilized and this provides a number of checks in developing the program. For example, both the fast and slow flux in both the  $s$  domain and the time domain should be symmetric. The extent to which they deviate from symmetry provides insight for determining possible areas of difficulty. It should also give an indication of the upper limit of the number of significant figures contained in  $\phi(x_i, s_j)$ . That is, if the  $s$  domain flux at symmetric points agrees to only three significant figures, the  $s$  domain flux cannot be presumed more accurate than this. As mentioned in the previous section this is an important consideration when returning to the time domain.

Figure 3 shows a plot of the Green's function for the fast group of the two-group, three region model given in problem one with  $\mu_{2\Sigma_2}^2 = .01$  and  $\mu_1^j = 1.0$  for all other combinations of  $i$  and  $j$ . The particular choice of  $\mu_{2\Sigma_2}^2$  is somewhat arbitrary and doesn't affect the fast group Green's function but it is necessary to use a value less than  $\Sigma_2^2$  of Table 1 in order to obtain the inverse of the thermal group boundary matrix. This inverse is necessary in determining the thermal group Green's function.

Theoretically the choice of  $\mu_2^2$  should not affect the final  $s$  domain solution. The solutions were observed, however to show some sensitivity to the choice of  $\mu_{2\Sigma_2}^2$ . It is felt that this sensitivity is due, at least in part, to the



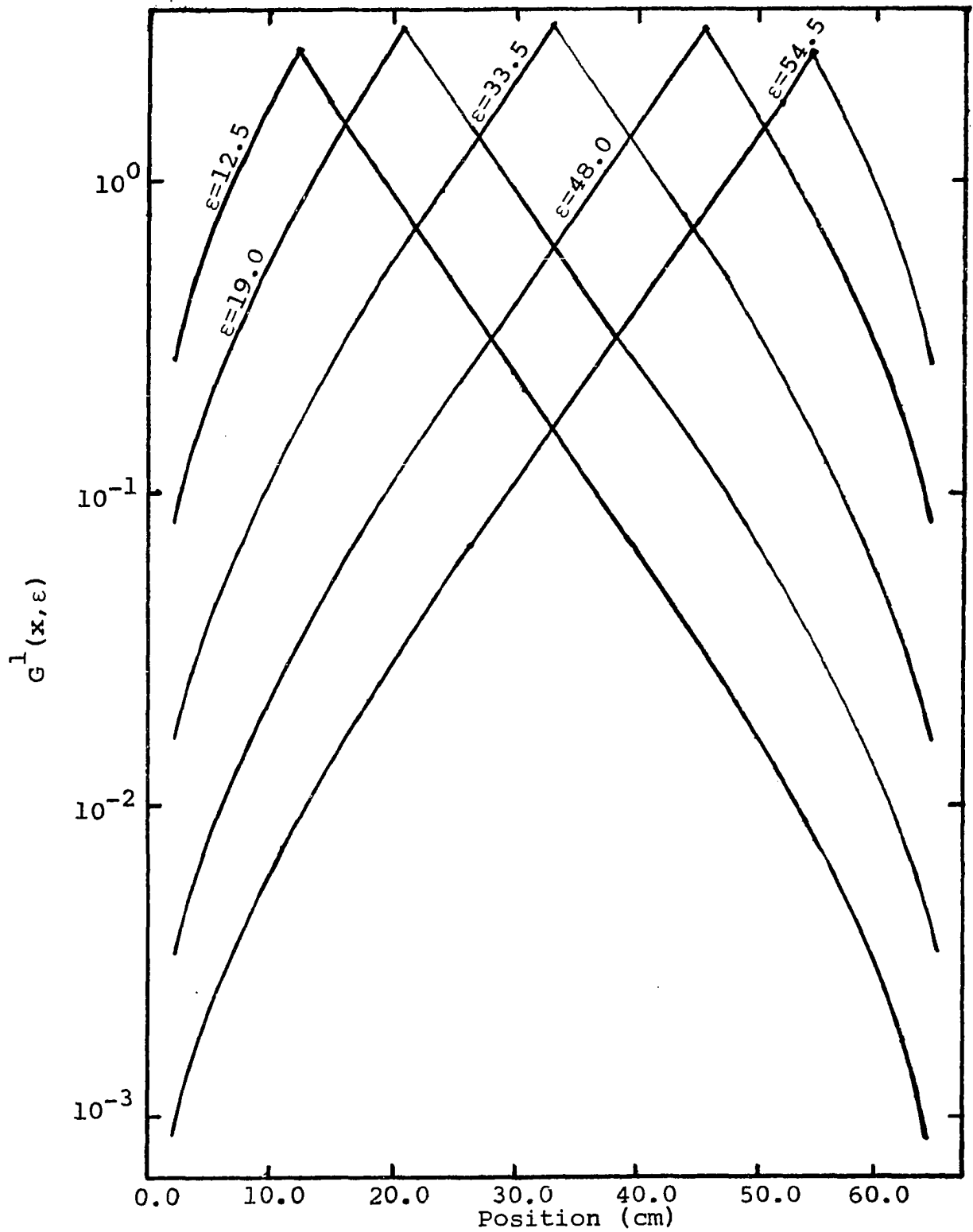


Figure 3. Fast group Green's function for problem one for several values of  $\epsilon$

grid spacing used in the analysis of this effect. It should be noted that inversions to the time domain with these solutions were unsuccessful. A full investigation of this sensitivity, using the finer grid spacing of the final analysis, was not made due to the increased computer cost associated with the finer spacing.

With the Green's functions determined for a particular grid, the driving function for each group may be obtained from Equation 27a. The initial steady state flux is obtained using a formulation from Glasstone and Edlund (16) along with the parameters given in Table 1. A plot of  $\bar{y}^1$  and  $\bar{y}^2$  is shown in Figure 4 for the configuration described previously. The weighting functions utilized in evaluating the integrals were obtained from the Handbook of Mathematical Functions (17). To avoid using negative weights, which occur in approximations involving more than eight points (i.e. approximating the integrand by a seventh order polynomial), those of higher order are broken into combinations of eight points or less. A nine point approximation is accomplished by two five point approximations and so on.

The Green's function and hence the driving function are independent of  $s$ . This need not be the case but it does avoid the necessity of recalculating them for each discrete value of  $s$  considered. In terms of the development in Sections III.A  $v$  is zero for all cases considered.

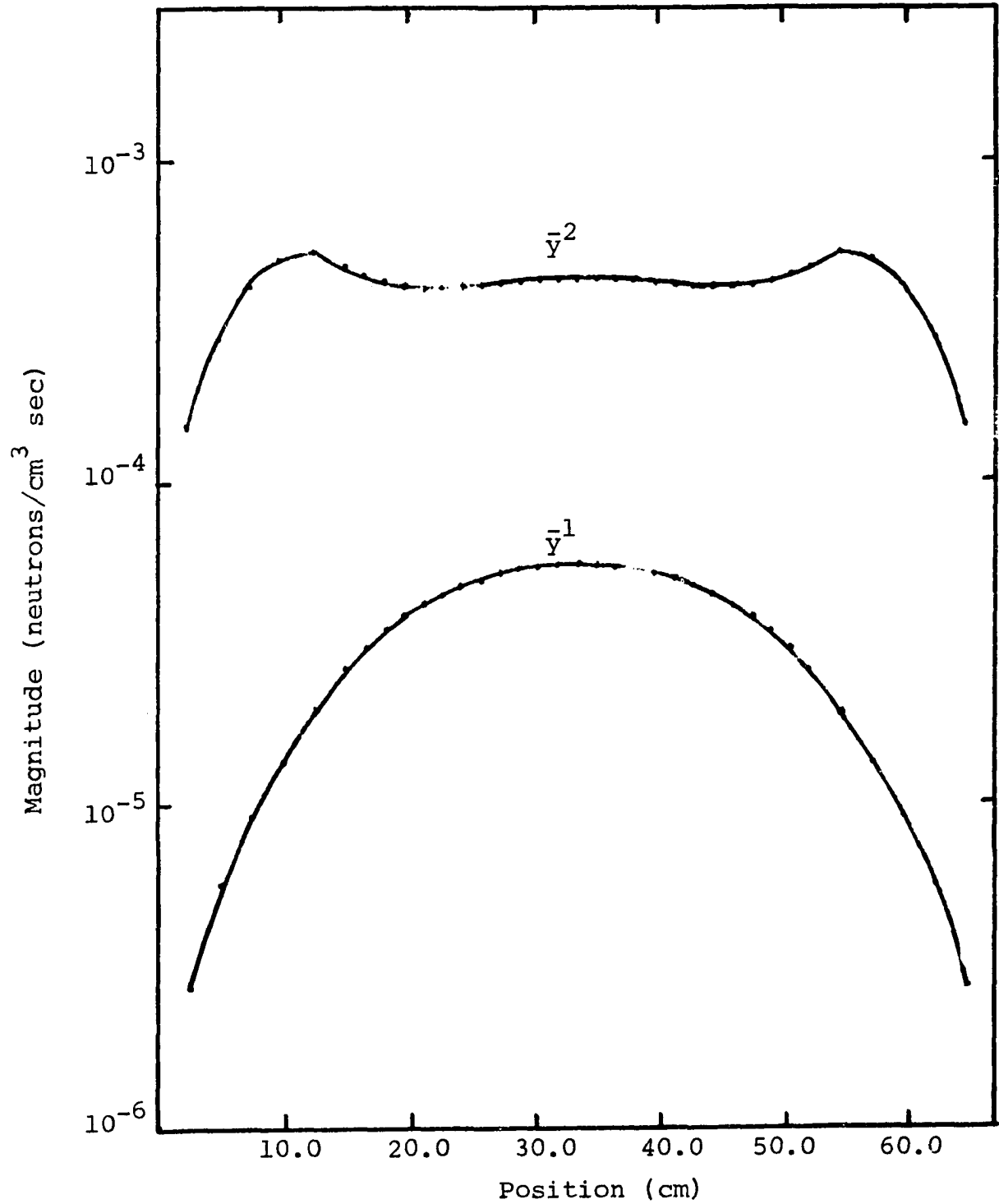


Figure 4. Driving functions for problem one

Problem two considers a perturbation in  $\Sigma_2^2$  of a four-region model obtained by inserting a boundary at 24 cm in the three region model above. The second region extends from 15 cm to 24 cm. This configuration presents a nonsymmetric perturbation. The locations of the discrete points arising from the space grids chosen for problems one and two are given in Table 2. In problem two the initial steady state parameters are the same as for problem one. As may be seen, most of the points for problem two coincide with a one cm grid. Ideally, one might obtain solution with the grid shown for problem two and then repeat the procedure for the grid with points every cm. Then  $\bar{y}$ ,  $\bar{\phi}(x_i, s_j)$ , and  $\bar{\phi}(x_i, t_j)$  could be compared at each point of correspondence to obtain an indication of the accuracy of each calculation. Obtaining  $\bar{\phi}(x_i, s_j)$  and  $\bar{\phi}(x_i, t_j)$  with the finer grid was entirely prohibitive from the standpoint of computer cost and only the determination of  $\bar{y}$  was accomplished. This comparison showed agreement to within  $\pm 2$  in the fourth significant figure in the worst cases and within  $\pm 2$  in the fifth significant figure for most cases. This indicates that the grid chosen adequately approximates the integrals involving the Green's functions and the initial steady state fluxes. No implications can be drawn as to the accuracy of  $\bar{\phi}(x_i, s_j)$  since the space dependence is different and an inversion of a matrix is involved, however, the results obtained for  $\bar{y}^1$  and  $\bar{y}^2$  were

certainly encouraging.

With the group Green's functions and the driving function determined, the  $s$  domain flux may be determined by Equation 28. The elements of  $GF(s)$  are defined in the same manner as described in section III.B.

Table 2. Space grids for problems one and two

Problem one		Problem two	
0.0	35.04	0.0	30.0
2.5	36.58	2.5	32.0
5.0	38.13	5.0	34.0
7.5	39.67	7.5	36.0
10.0	41.21	10.0	38.0
12.5	42.75	12.5	40.0
15.0	44.29	15.0	42.0
16.54	45.83	16.0	44.0
18.03	47.38	17.0	46.0
19.63	48.92	18.0	48.0
21.17	50.46	19.0	50.0
22.71	52.0	20.0	52.0
24.25	54.5	21.0	54.5
25.79	57.0	22.0	57.0
27.33	59.5	23.0	59.5
28.88	62.0	24.0	62.0
30.42	64.5	26.0	64.5
31.96	67.0	28.0	67.0
33.5			

## V. RESULTS AND DISCUSSION

Five variations of the two problems previously discussed will be considered in this section. For convenience they are listed in Table 3 and will be referred to by case number in the discussion that follows.

Table 3. Pertinent parameters for variations of problems one and two considered

Case number	Problem	Perturbation ( $\delta\Sigma_2^2$ )	Time scale ( $\alpha$ )	$\mu^2\Sigma^2$ in core	All other $\mu_i$
1	one	-.003	.001	.01	1.0
2	one	.003	.001	.01	1.0
3	two	-.006	.001	.01	1.0
4	two	-.006	.002	.01	1.0
5	two	-.006	.010	.001	1.0

The  $s$  domain solutions are obtained by inserting  $s = P/a$  into Equation 28 for  $p = 1, 2, \dots, N$  and performing the inversion. The scale factor  $\alpha$  affects both the time scale and the polynomial expansion as shown in section III.A. Thus the determination of the  $s$  domain solutions are governed by time domain considerations.

As the  $s$  domain solutions have no basis for comparison, only the thermal group of case 4 will be shown. The fast

group solutions are uninteresting in both the  $s$  domain and time domain as far as space dependence for the problems considered as they deviate little from the steady state shape. Figure 5 gives the first four  $\phi^2(x,s)$  corresponding to  $p = 1,2,3,4$  for case 4. This set is typical of all sets of  $s$  domain solutions in that as  $p$  and hence  $s$  increase, the magnitude of the  $s$  domain flux decreases and the difference in the magnitude of solutions for successive values of  $p$  also decreases. If this were not the case, inversion to the time domain would appear to be impossible. This statement is in the nature of speculation and is offered without proof but this would seem to parallel the case of a divergent series. The mere fact that a set of  $s$  domain solutions exhibit this trend is no guarantee an inverse can be obtained. Generally, the  $s$  domain solutions give no indication as to whether or not an inversion to the time domain can be obtained.

As a result of the Gaussian Quadrature utilized in the inversion, the discrete times for which the flux are obtained are fixed by  $t_i = -\alpha \ln(r_i)$  where  $r_i$  are the roots of the Legendre polynomial of order  $N$ . The values of  $\ln(r_i)$  for  $N = 3,4,5,6$  are given in Table 4.

The tendency of the values of  $t_i$  to cluster at the lower end of the time range makes plotting space profiles for all values of  $t_i/\alpha$  difficult. Adding to the difficulty is the spacial scatter which will be noted in the plots which follow.

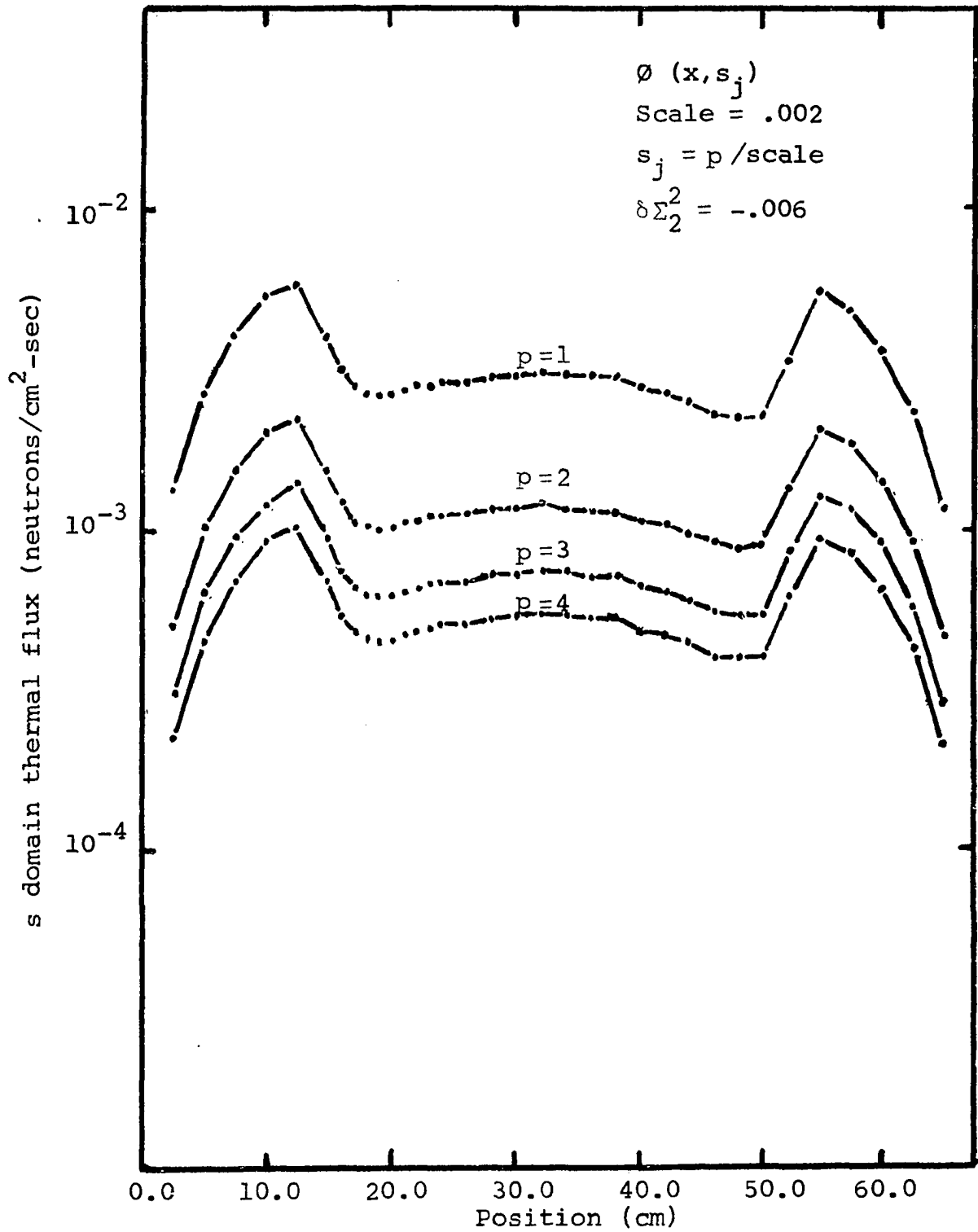


Figure 5. s domain thermal flux for case 4



Table 4. Values of  $t_i/\alpha = \ln(r_i)$ 

N	$t_1/\alpha$	$t_2/\alpha$	$t_3/\alpha$	$t_4/\alpha$	$t_5/\alpha$	$t_6/\alpha$
3	2.183	0.693	0.120	x	x	x
4	2.667	1.109	0.400	0.0720	x	x
5	3.050	1.466	0.693	0.262	0.048	x
6	3.388	1.776	0.966	0.479	0.186	0.034

Plots of the space profiles will be restricted to the one at time  $t_i/\alpha$  for as many values of N as inversions have been obtained. In addition, the fast flux space profiles are uninteresting and except for case 4 will not be given.

Plots of the time dependent flux shape at the space point of maximum flux in the core will be given for all  $t_i/\alpha$  of all N for which time inversions were obtained. The WIGLE-40 solution at this same point will be given for comparison.

For case 1, inversions for N = 3,4 were all that could be obtained. These are given in Figure 6 along with the steady state initial solution and a profile from WIGLE-40. The spacial scatter is emphasized by connecting points with straight lines as opposed to using a fitted curve. The choice of  $\alpha = .001$  was made to obtain solutions over a time range of zero to slightly over three milliseconds. There is

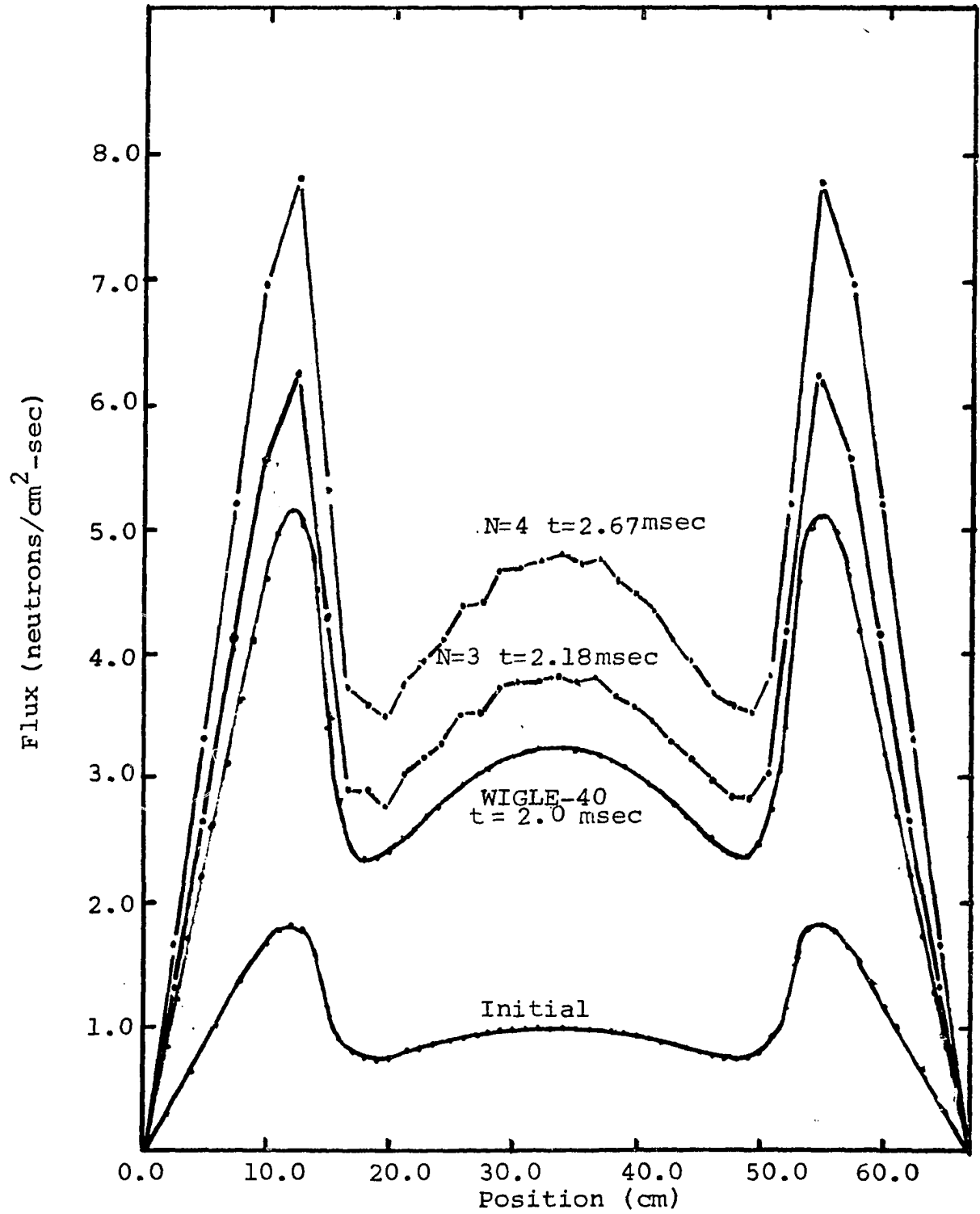


Figure 6. Thermal group space profiles from case 1

some basis for feeling that the time scale chosen affects the quality of the space profiles as well as the order of inversion which may be obtained and the degree to which agreement with WIGLE-40 is obtained. This will be demonstrated in comparison of cases three and four.

The time dependence of both the fast and slow flux along the centerline is given in Figure 7. The agreement at times  $t_1/\alpha$  for  $N = 3,4$  is reasonably good but considerable scatter is evident at times  $t_i/\alpha$ ,  $i > 1$ .

The time dependence of the fast and slow center line flux from case two is given in Figure 8. A smoother time dependence is noted as the scatter is much less for  $t_i/\alpha$ ,  $i > 1$ . Agreement with WIGLE-40 is not as good, however, for times  $t_1/\alpha$  and  $N = 3,4$  as for case one. In addition the space profile (not shown) exhibits more scatter in case two than in case one.

No attempt was made to improve the quality of the solutions for the symmetric case. It was felt that a nonsymmetric perturbation would provide more of a test of the ultimate usefulness of the general approach and would be more interesting.

A plot of the space profile for  $N = 3$  at  $t_1/\alpha$  is given in Figure 9 for case 3. The profile for  $N = 4$  at  $t_1/\alpha$  displayed considerably more scatter and was not sufficiently displaced from the one given to avoid some overlapping so

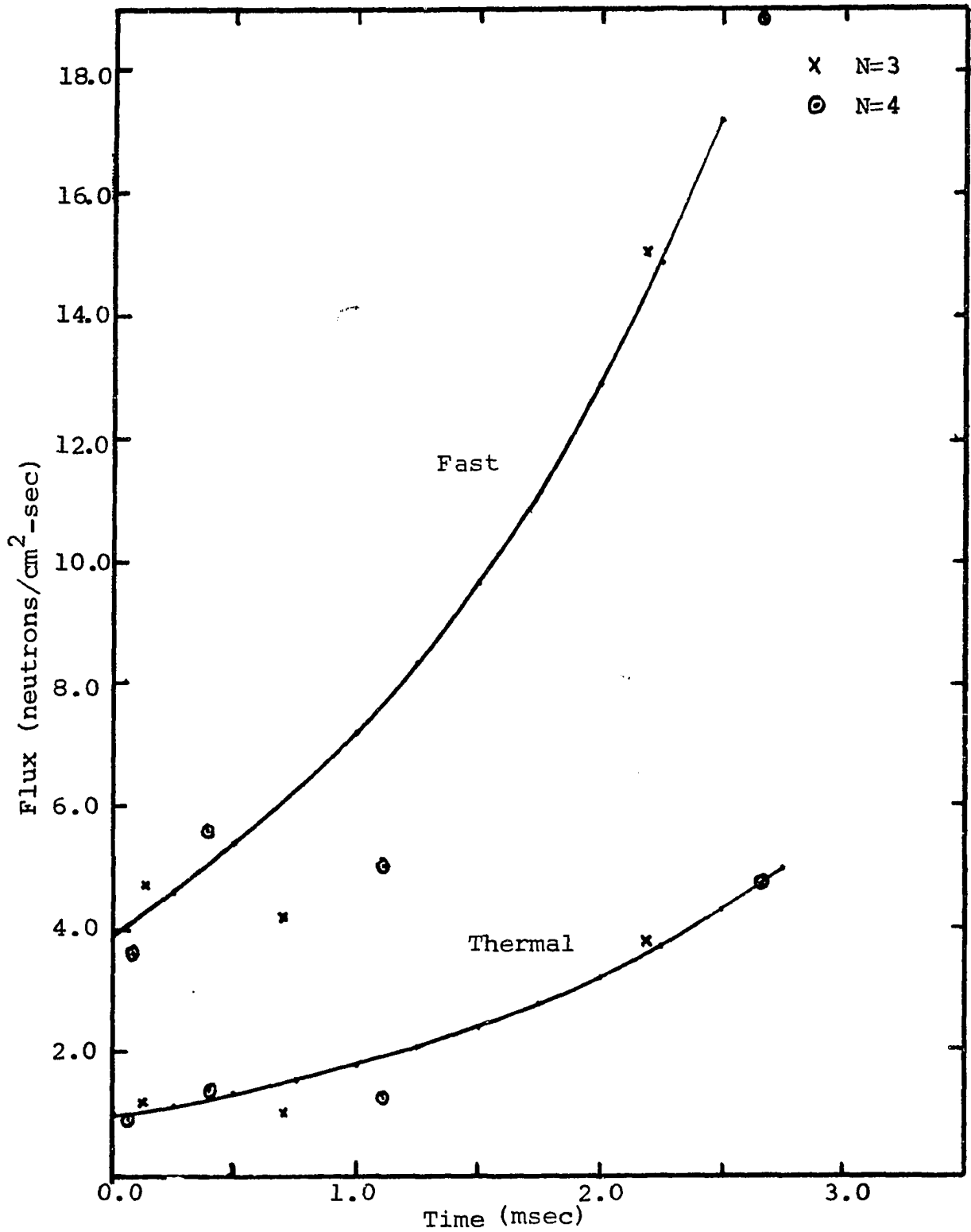


Figure 7. Time dependent fast and thermal centerline flux for case 1

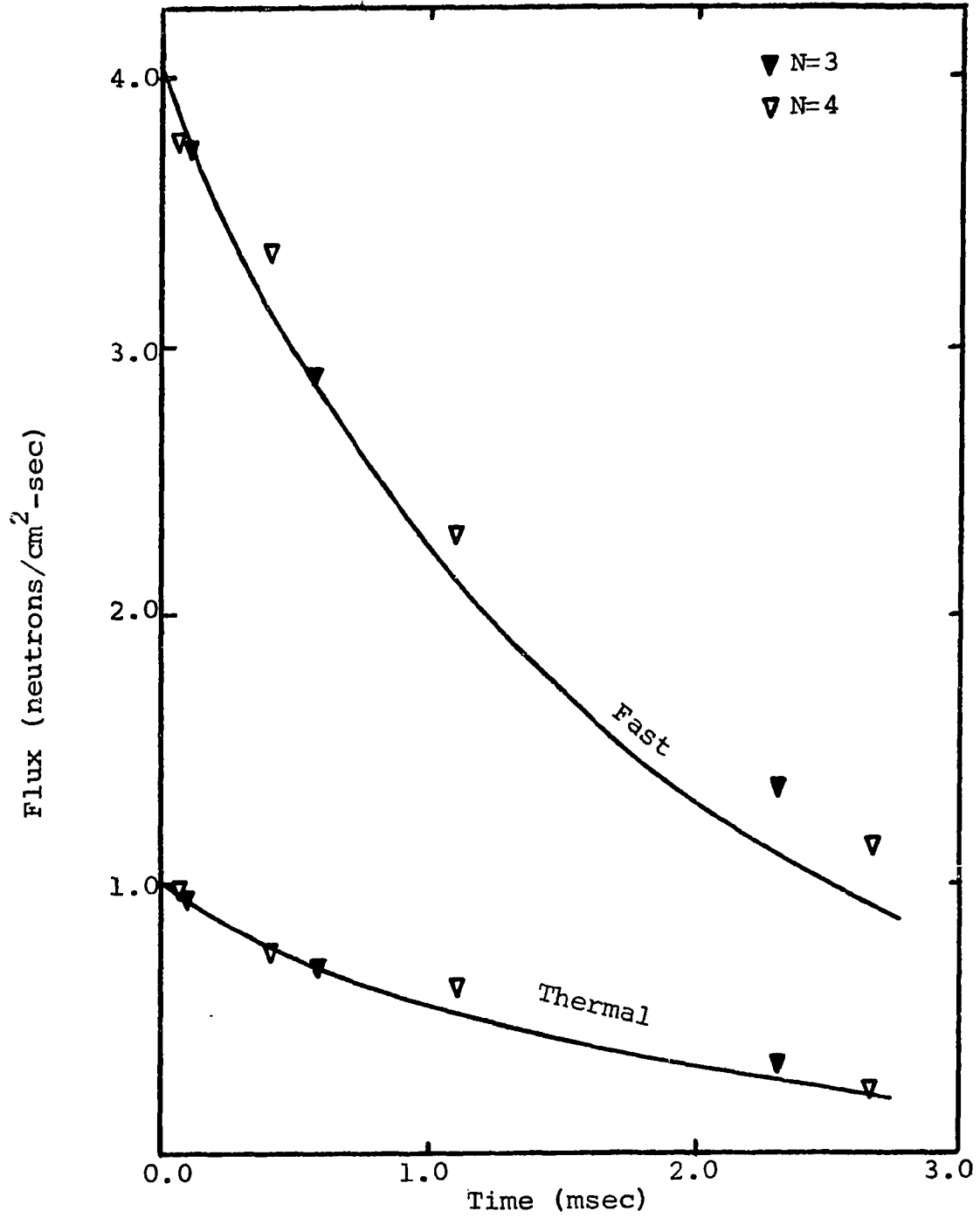


Figure 8. Time dependent fast and thermal centerline flux for case 2

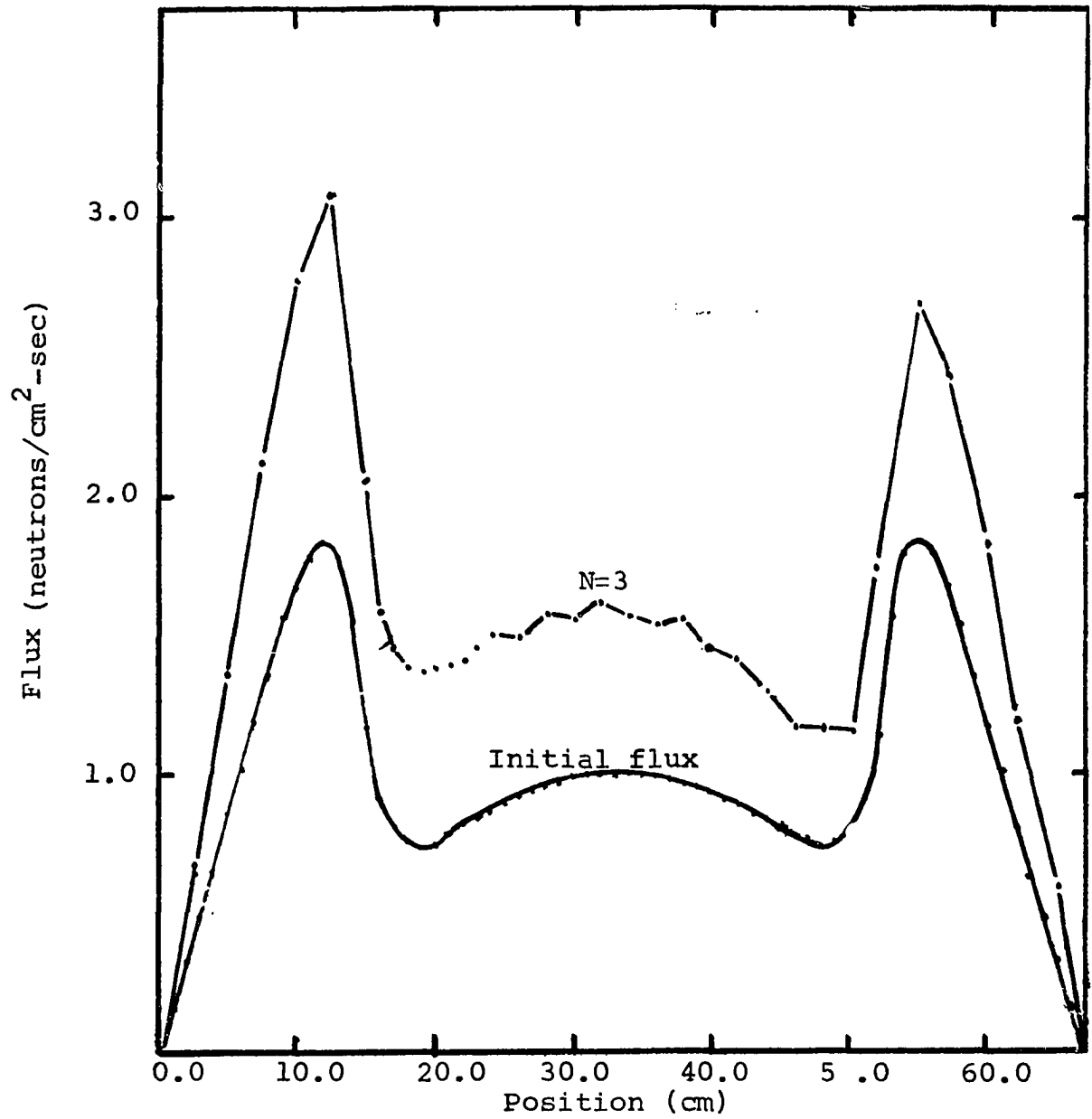


Figure 9. Thermal group flux for case 3, N=3

it is not shown. The time dependence at  $x = 32$  cm is given in Figure 10 along with the WIGLE-40 solution for the same point. The agreement is not especially good and scatter is evident.

Case four concerns the same problem as case three with a scale factor twice as large. Inversions were obtained for  $N = 3, 4, 5, 6$  and the profiles associated with time  $t_1/\alpha$  for each  $N$  are shown in Figure 11 (thermal group) and Figure 12 (fast group). They are seen to be considerably smoother than those of problem three with the smaller time scale. The time dependence of the thermal flux at  $x = 32$  cm is given in Figure 13. It is seen that the WIGLE-40 solution is increasing at a faster rate. The technique under consideration has been checked with zero perturbation and found to yield a constant steady state output. A zero perturbation was inserted into WIGLE-40 and the results for both the fast and slow flux are plotted in Figure 14. In 6.0 msec an increase of 5% is noted. At 6.0 msec in Figure 13, the flux as obtained from WIGLE-40 is about 5% higher than that obtained by the method under investigation. This might approximately account for the differences between the two solutions.

Case 5 which represented changes in  $a$ ,  $\mu_2^2 \Sigma_2^2$ , and  $\mu_3^2 \Sigma_3^2$  was unsuccessful in that no inversions to the time domain were accomplished.

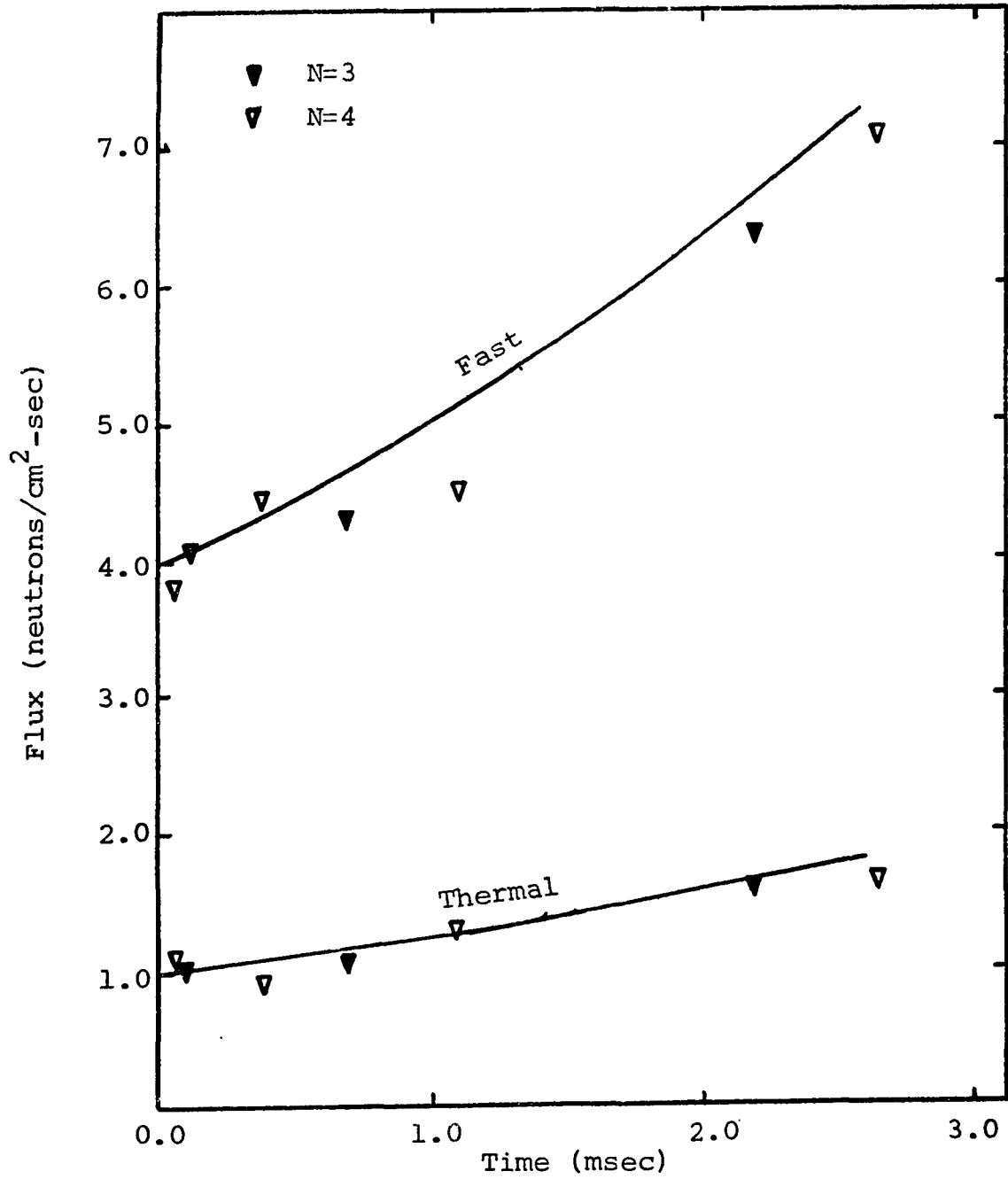


Figure 10. Time dependent flux for case 3 at  $x = 32.0$  cm



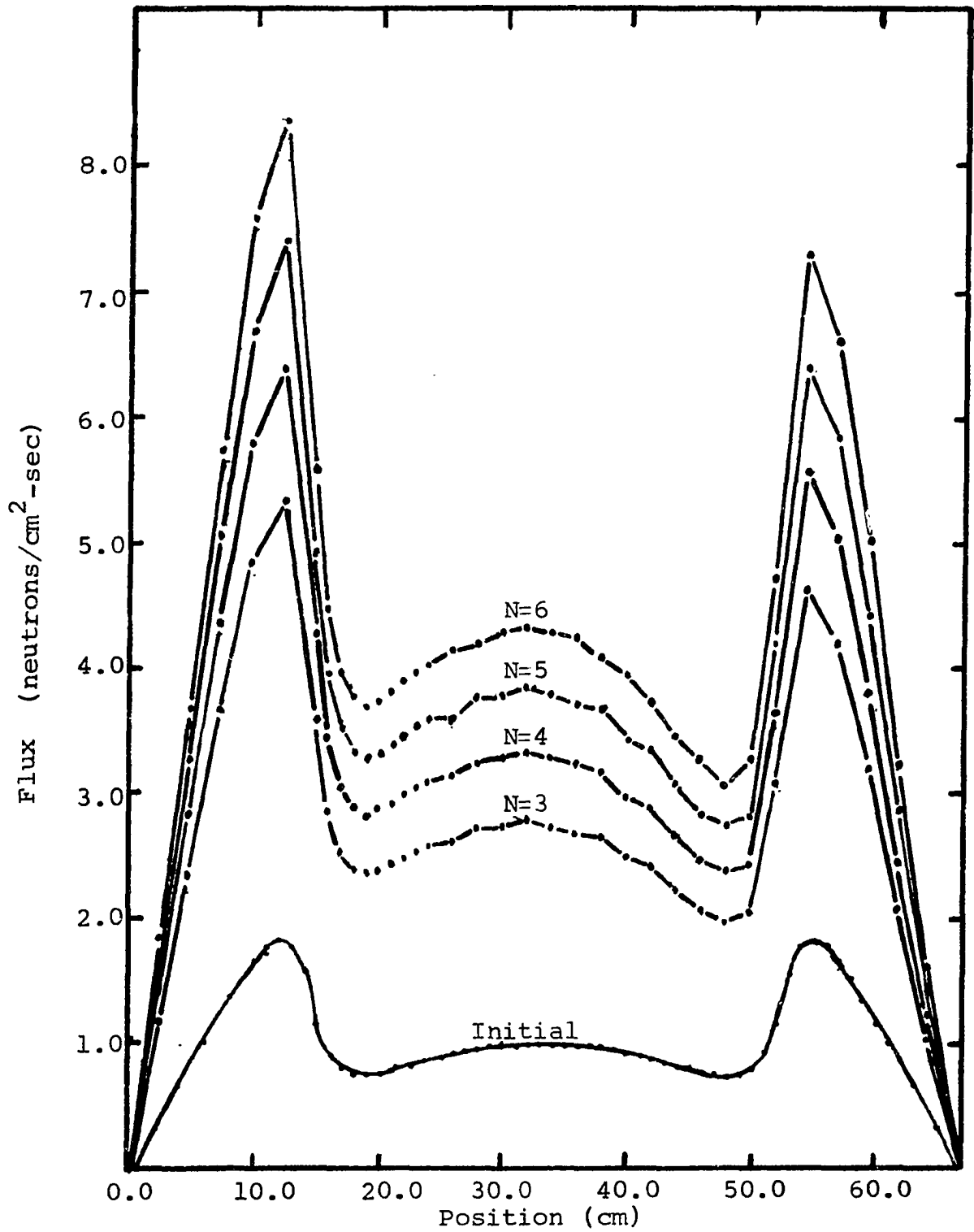


Figure 11. Thermal group flux for case 4,  $N = 3, 4, 5, 6$

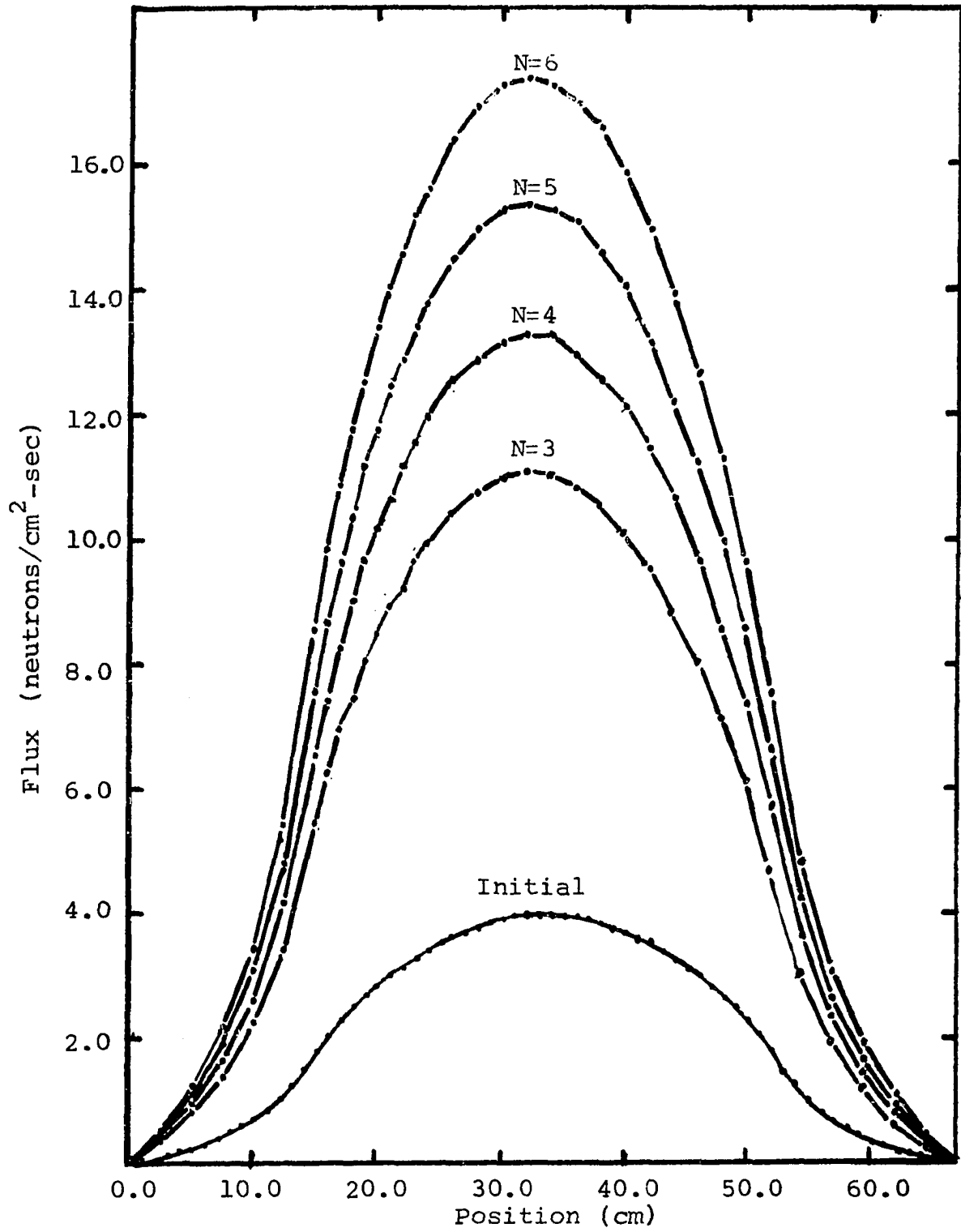


Figure 12. Fast group flux for case 4

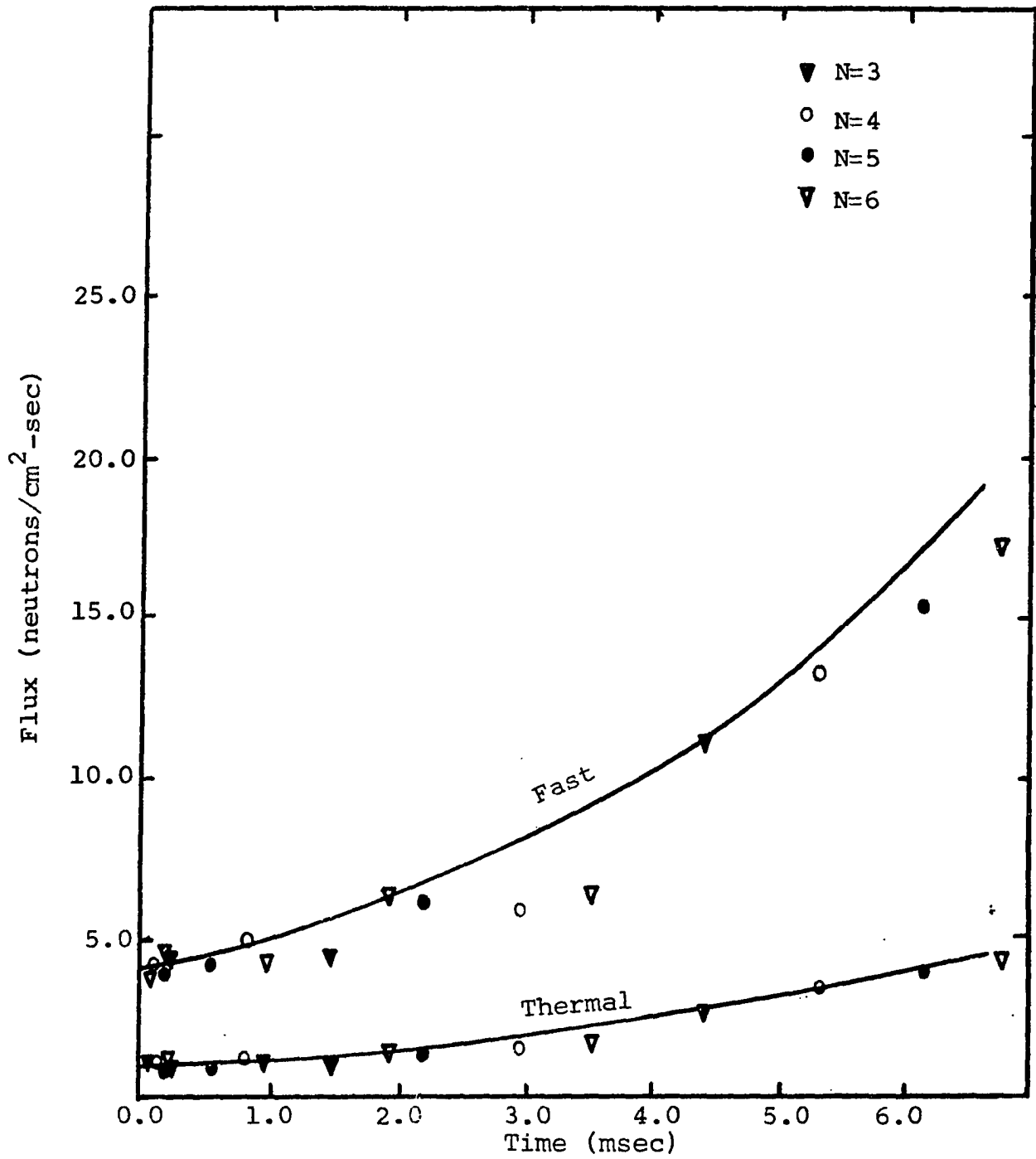


Figure 13. Time dependent fast and thermal flux at  $x = 32$  cm

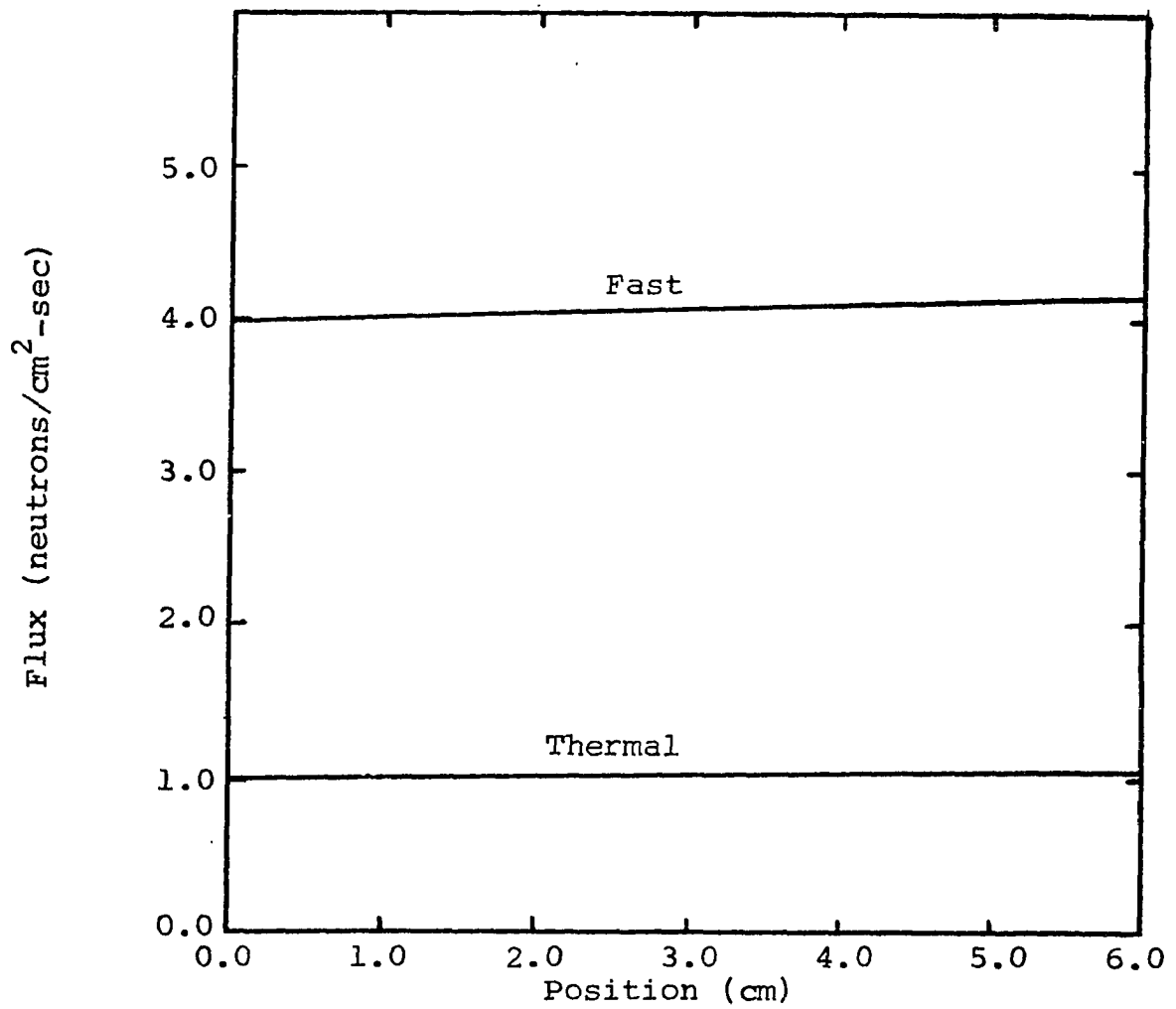


Figure 14. Thermal and fast flux (WIGLE-40),  $\delta\Sigma = 0.0$ , at  $x = 32.0$  cm

The results obtained demonstrate that an approach of this type is feasible. There can be no doubt that the technique needs further investigation and refinement. A number of questions remain unanswered. In particular the full effect of the values of  $\alpha$  and  $\mu_2^2$  on the ultimate solution was not established. The fact that  $\mu_2^2$  had an effect on the s domain solutions for grids with relatively wide spacing is not surprising as the approximations of the integrals would not be as good as for grids with finer spacing. Inversion to the time domain could not be accomplished in these cases.

The fact that the quality of the solution depends on the time scale is unfortunate since this limits the range over which solutions may be obtained. This could be overcome to a large extent, however, if the solutions were sufficiently accurate to allow using the space profile from  $t_1/\alpha$  from the highest order inversion obtained as the initial flux for another set. This would require a large degree of confidence in the technique as it causes a propagation of errors. An inexpensive method of establishing a "best value" of the scale factor would also be highly desirable.

The top priority at this point would, however, have to be the reduction of computer cost in obtaining these solutions. Since the inversion associated with Equation 28 represents by far the largest expense, it must come under close scrutiny. One means of dispensing with it would be to use a finite difference technique to obtain the s domain solutions.

Another possibility would be to leave the  $s$  dependent part of the matrix on the right hand side of Equation 26. This would change Equation 28 to one of the form

$$\bar{\phi}(s) = [I - GF]^{-1} D(s) \bar{\phi}(s) + [I - GF]^{-1} \bar{y}$$

thus the matrix  $[I - GF]$  is not  $s$  dependent and need be determined only once in obtaining the set of  $s$  domain solutions. This creates an iterative problem which could be solved by conventional techniques provided the absolute value of the spectral radius associated with the matrix  $[I - GF]^{-1} D(s)$  was less than one.  $D(s)$  is a block diagonal matrix with multiples of  $s$  in the blocks.

It is also possible that the use of Laguerre Polynomials in place of Legendre Polynomials in the inversion to the time domain would yield a more powerful inversion technique. In any case the use of the Laplace transform in obtaining solutions to the multigroup diffusion equations does appear to have possibilities.

## VI. TOPICS FOR FURTHER STUDY

Several topics have been suggested in the previous section. The possibility of using Laguerre Polynomials to obtain the inversion to the time domain could be investigated. These polynomials are orthogonal to the weighting function over the interval  $(0, \infty)$  and appear well suited to the Laplace transform.

Two alternative methods for obtaining the  $s$  domain solutions are suggested in the form of a finite difference technique and an iterative approach. These should be quicker and hence less expensive on the computer.

If the current inversion scheme is to be used, the effect on the scale  $\alpha$  needs further investigation. If the iterative Green's function approach is pursued, the effect of  $\mu_i^j$ , if any, should be established for the grid used. If sufficient funding is available, the effect of these parameters might be established with the approach used here. It would be useful in the iterative approach to have these effects already established.

## VII. LITERATURE CITED

1. Bellman, R. E., Kalaba, R. E. and Lockett, J. Numerical inversion of the Laplace transform. New York, N.Y., Elsevier Publishing Co. 1966.
2. Foderaro, A. and Garabedian, H. L. A new method for the solution of group diffusion equations. Nuc. Sci. and Eng. 21: 536-549. 1965.
3. Kaplan, S. The property of finality and the analysis of problems in reactor space-time kinetics by various model expansions. Nuc. Sci. and Eng. 9: 357-361. 1961.
4. Foulke, L. R. and Gyftopoulos, E. P. Application of the natural mode approximation to space-time reactor problems. Nuc. Sci. and Eng. 30: 419-435. 1967.
5. Harris, D. R., Kaplan, S. and Margolis, S. G. Modal analysis of flux tilt; transients in a nonuniform-reactor. Am. Nucl. Soc. Trans. 2: 178-179. 1959.
6. Dougherty, D. E. and Shen, C. N. The space-time neutron kinetic equations obtained by the semi-direct variational method. Nuc. Sci. and Eng. 13: 141-148. 1962.
7. Carter, N. E. and Danofsky, R. A. The application of the calculus of variations and the method of Green's functions to the solution of coupled core kinetics equations. In Chezem, C. G. and Kohler, W. H., editors. Conf. Coupled Reactor Kinetics, College Station, Texas, Jan. 1967. Pp. 249-269. College Station, Texas, The Texas A and M Press. 1967.
8. Carter, N. E. Solution of space-time kinetic equations for coupled core nuclear reactors. Unpublished Ph.D. thesis. Ames, Iowa, Library, Iowa State University of Science and Technology. 1967.
9. Yasinsky, J. E. On the application of time-synthesis techniques to coupled core reactors. Nuc. Sci. and Eng. 32: 425-429. 1968.
10. McFadden, J. H. Solution of the space-time kinetics equations for a reflected slab reactor. Unpublished Ph.D. thesis. Ames, Iowa, Library, Iowa State University of Science and Technology. 1968.



11. Yasinsky, J. B. On the application of time-synthesis techniques to coupled-core-type reactors. Am. Nucl. Soc. Trans. 10: 570-571. 1967.
12. Cadwell, W. R., Henry, A. F., and Vigilotti, A. J. WIGLE. A program for the solution of the two-group space-time diffusion equations in slab geometry. U.S. Atomic Energy Commission Report WAPD-TM-416 (Westinghouse Electric Corp. Atomic Power Division, Pittsburgh, Pa.). 1964.
13. Radd, M. E. WIGLE-40, A two-group, time-dependent diffusion theory for the IBM-7040 computer. U.S. Atomic Energy Commission Report IDO-17125 (Phillips Petroleum Corp. Atomic Energy Division, Idaho Falls, Idaho). 1965.
14. Andrews, J. Barclay, II and Hansen, K. F. Numerical solution of the time-dependent multigroup diffusion equations. Nuc. Sci. and Eng. 31: 304-313. 1968.
15. Loewe, W. E. Space-dependent effects in the response of a nuclear reactor to forced oscillations. Nuc. Sci. and Eng. 21: 536-549. 1965.
16. Glasstone, S. and Edlund, M. C. The elements of nuclear reactor theory. New York, N.Y., D. Van Nostrand Co., Inc. 1952.
17. Abramowitz, M. and Stegun, I. A., eds. Handbook of mathematical functions with formulas, graphs, and mathematical tables. U.S. National Bureau of Standards Applied Mathematics Series 55: 886-887. 1964.

## VIII. ACKNOWLEDGMENTS

The author wishes his appreciation to Drs. Glenn Murphy, Richard A. Danofsky, Alfred F. Rohach, Larry B. Coady, and James W. Nilsson who formed his graduate committee. Special thanks are due Dr. Richard A. Danofsky for a number of enlightening consultations during the course of this investigation.

The author wishes to thank the Atomic Energy Commission for the fellowship under which the work was accomplished.

The author is deeply indebted to his wife Carole for her encouragement and financial support throughout his college career and to his children Joan, Bill, and John for their patience and understanding.